A MAGNETICALLY SUSPENDED

LINEARLY DRIVEN CRYOGENIC REFRIGERATOR*

F. Stolfi, M. Goldowsky,
J. Ricciardelli and P. Shapiro
Philips Laboratories
Briarcliff Manor, New York 10510

ABSTRACT

This paper describes a novel Stirling cycle cryogenic refrigerator which was designed, fabricated and successfully tested at Philips Laboratories. The prominent features of the machine are an electro-magnetic bearing system, a pair of moving magnet linear motors, and clearance seals with a 25 μm radial gap. The all-metal and ceramic construction eliminates long-term organic contamination of the helium working fluid. The axial positions of the piston and displacer are electronically controlled, permitting independent adjustment of the amplitude of each and their relative phase relationship during operation. A simple passive counterbalance reduces axial vibrations. The design of the refrigerator system components is discussed and a comparison is made between performance estimates and measured results.

INTRODUCTION

In 1978, Philips Laboratories proposed to design, fabricate and test a cryogenic refrigerator for spaceborne applications, under the sponsorship of the NASA Goddard Space Flight Center. Drawing on expertise developed at Philips over the last 40 years, the unit was based on the Stirling cycle but incorporated many novel electromechanical features which extended the operational life of the machine greatly beyond that of units built in the past. The ultimate goal is a system capable of producing 5 W of refrigeration at 65°K for 5 years or longer. The purpose of the first model, which was successfully tested in March 1982, was to prove the viability of the technology (Ref. 1).

(*) This work was performed under NASA Goddard Contract number NAS5-25172.

SYSTEM DESCRIPTION

GENERAL ASPECTS

The novelty of the refrigerator stems from the use of active magnetic bearings, clearance seals, and an electronically controlled direct-drive linear motion. The use of these three basic features leads to a design promising long mechanical life, comparatively high electromechanical efficiency and high thermo-dynamic stability. In short, it produces a refrigerator which is compatible with the ultimate intended spaceborne applications.

With active magnetic reciprocating bearings, the moving elements of the refrigerator are electro-magnetically suspended in small annular gaps. Friction, wear and particle generation are eliminated since there is no mechanical contact. Further, this approach allows the refrigerator to be made from only metal and ceramic components. There is no need for lubrication, either wet or dry. With the complete absence of organic materials and the associated contamination of the working gas, a principal cause of thermal degradation is avoided.

Clearance seals, an apparent contradiction in terms, is the designation given to the 25 μm radial gaps around certain sections of the moving elements. Since the amount of gas which can flow through these long narrow passages is limited, they effectively form dynamic pressure seals. This type of seal, accomplished without the use of organic materials or mechanical contact eliminates a traditional life limiting component in Stirling machines.

By using moving-magnet linear motors as the drive mechanism, linkages and flexing power leads are eliminated. The result is a design with high electro-mechanical efficiency, long life and high reliability. Since the motors are controlled with an electronic control system, the user has complete flexibility in adjusting the amplitude and the frequency of the linear motions. This gives the system a high degree of mechanical and thermodynamic versatility.

The development of the magnetic bearings and linear motors included the design, construction and use of dedicated test fixtures. The refrigerator is not an optimal test vehicle for these components since their individual design parameters could not be independently evaluated. However, since the bearings and motors are meant to perform a specific task, the test fixtures had to simulate the refrigerator as closely as possible. In the case of the bearings, this meant a fixture machined to close tolerances using materials and joining techniques equivalent to those used in the refrigerator. For the motor, this meant a fixture which utilized a gas spring and an air bearing.

Following a description of the refrigerator, the design and testing of the major subsystems (the bearings, linear motors, axial control system and

passive countermass) will be discussed. The paper concludes with the description and results of several thermodynamic parametric tests; work that is currently in progress.

CONFIGURATION

The cryogenic refrigerator, shown in cross section in Figure 1, is composed of three major sections. In the displacer section, gas is cyclically shuttled from the cold expansion end to the rear compression section which is held at ambient temperature with the aid of a water jacket/heat exchanger. In the second major section, the gas is expanded and compressed through the action of a piston. Finally, the third section contains a spring-mass passive counterbalance, which minimizes axial vibrations when tuned to the refrigerator running frequency. The piston and displacer elements are supported on magnetic bearings, the countermass, on leaf springs. A photograph of the refrigerator is shown in Figure 2.

Displacer Subassembly

The displacer section is shown in detail in Figure 3. Helium gas, the working fluid, is free to flow from the expansion space at the 65°K flange, through the heat exchanger, which is maintained at 300°K with a water jacket, to the compression space in the piston section. A copper cap at the cold end serves as a heat exchanger and minimizes cyclic thermal variations. A moving regenerator maintains the temperature gradient along the length of the cold finger by storing heat energy in one half of the cycle to release it in the other half. The magnetic bearings and radial position transducers shown in Figure 3, form the first two clearance seals, forcing the helium to flow through the regenerator and through the heat exchanger. The axial motion of the displacer is driven by a moving magnet linear motor and transduced with a linear variable differential transformer (LVDT). The LVDT, described in greater detail in Section 5, requires no mechanical contact with the moving displacer.

Piston Subassembly

The piston section is shown in detail in Figure 4. The magnetic bearing on the left forms the third and final clearance seal; its function is to maintain the cyclic pressure in the compression space. The additional magnetic bearing at the rear of the piston supports the shaft but does not form a seal. The hollow vented piston shaft and the large volume in the center of this section constitute a buffer space for helium gas. As in the displacer, the axial motion control entails the use of a moving magnet linear motor and an LVDT.

Since there is no physical connection between the piston and displacer (such as a crankshaft and connecting rods), the refrigerator produces cold only through the action of an electronic control system which regulates the

amplitude and phase of each element. The displacer must lead the piston by a specific phase angle (about 60°) so that the gas is principally located in the compression (300°K) section when the piston compresses and in the expansion (65°K) section when the piston expands. Thermodynamic stability is achieved only if this phase and amplitude relationship is accurately maintained.

Countermass Subassembly

The countermass is shown in cross section in Figure 5. It passively reciprocates in vector phase opposition to the combined piston and displacer momentum when the coil spring/moving mass resonance is tuned to the refrigerator running frequency. Since the three subassemblies are bolted together on a common centerline, the action of the countermass minimizes the axial vibration of the refrigerator housing. The leaf springs provide radial support, adding little damping to the system. The countermass is tuned to the refrigerator operating frequency by changing the tuning mass shown in Figure 5.

MAGNETIC BEARINGS

DESCRIPTION

The configuration of the magnetic bearings is shown diagrammatically in Figure 6. Each ferromagnetic pole piece exerts a radial attractive force on the reciprocating shaft when current is applied to its coil winding. By situating poles diametrically opposite, one end of the shaft may be controlled in one plane by regulating the current in each pole (see Fig. 7). By positioning sets of poles at orthogonal planes on each end of the shaft, the shaft may be suspended (centered in the bore).

The radial position of the shaft is transduced with eddy current sensors. The eddy current probe consists of a flat coil which is situated parallel to the sensed shaft. By applying a high frequency voltage to this coil, eddy currents are generated in the shaft and the magnitude and phase of these eddy currents change as the magnetic air gap changes. The probe thus provides a dynamic measurement of shaft position. The probes are mounted differentially so that temperature-induced drift is substantially reduced.

FABRICATION

In the refrigerator, three of the magnetic bearings also form clearance seals. The dual nature of these sections, and the use of only metal and ceramic materials, means that special fabrication techniques are required in the construction. The 25 μm gap between the shaft and the housing requires the use of materials with high dimensional stability. Each cross section is radially symmetric to minimize thermal stresses. The ferromagnetic pole

pieces for the bearings are brazed hermetically to the housing wall, and the optimized magnetic properties of the pole pieces are still maintained. The eddy current probes are mounted behind ceramic windows with a thickness of 1 mm to prevent the organic insulation and potting compound used in their construction from contacting the working gas. Finally, the thermal expansions of the titanium alloy used for the housing, the iron alloy chosen for the pole pieces and the ceramic in the windows are closely matched, to prevent thermal stress and distortion.

BEARING CONTROL SYSTEM

The bearing electronic control system is shown diagrammatically in Figure 8. The pole piece magnetics are highly nonlinear: the force is porportional to the square of the current and inversely proportional to the square of the air gap. The electromagnetic field in the iron is influenced by the effects of eddy currents, hysteresis and magnetic saturation. The shaft dynamics includes a damping force caused by the gas squeeze film in the 25 μm gap.

The bearing controller can be modeled as a linear feedback regulator if it is assumed that the variations in the radial displacement and differential current are small about their nominal values. A reference center position of zero volts is compared to the transduced position voltage from the eddy current sensors. Any difference between these two signals regulates the current in the diametrically opposite pole pieces so as to reduce the error. The compensator is designed to provide large restoring signals for small errors over a wide frequency band in spite of the nonlinear nature of the magnetics and dynamics. A current amplifier is used so that the destabilizing phase shifts caused by the coil inductance and eddy currents are minimized.

TEST RESULTS

The magnetic bearing test fixture is shown in Figure 9. A linear shaker was connected to the center of the suspended shaft through a piezoelectric force transducer. The radial position of the shaft was dynamically measured with the eddy current sensors. The diameter of the shaft, the width and length of the clearance seal area, and the method by which the ferromagnetic materials were joined were chosen to simulate the piston section of the refrigerator.

The measured dynamic "stiffness" of the magnetic bearing is shown in Figure 10; the static load data in Figure 11. The dynamic stiffness increases at 200 Hz because the shaft inertia dominates the response. The test fixture also facilitated the development of the bearing electronic control system; Table 1 gives a summary of the control system and radial position sensor performance in refrigerator operation. This work demonstrated the feasibility of using linear magnetic bearings in the refrigerator, since, as the data shows, they exhibit a higher stiffness than many mechanical bearings.

LINEAR MOTORS

DESCRIPTION

The principle of operation of the linear motors used in this refrigerator is similar to that of the actuators used in most loudspeakers (Fig. 12 is an expanded view of the piston motor shown in Fig. 4). Permanent magnets, rather than a field coil, establish a steady magnetic flux field. The current through the coil interacts with the flux to produce a force between the coil and the permanent magnet. Since the flux is oriented radially and the coil is wound circumferentially, the force is directed along the axis of the motor, producing linear motion.

Figure 12 shows an inner and an outer coil section for each of the two "motor sections". The presence of substantial non-magnetic gaps (the coils) on each side of the magnet rings reduces the radial force generated between the moving-magnet armature and the stationary iron stator rings. Otherwise, these side forces can represent a significant load for the magnetic bearings.

An additional feature of this motor design is the ability to hermetically isolate the helium working gas from all possible sources of organic contamination. The hermetic seal is made by welding thin-walled titanium cans over the magnets and the coils. If the cans are relatively thin (0.3 mm), the reduction in the motor efficiency will be small.

Figure 13 is a photograph of the complete motor, with the armature mounted to the piston shaft and the stator assembly ready for insertion into the housing of the piston motor.

The displacer motor shown schematically in Figure 14 functions in the same manner as the piston motor. The geometry is somewhat different in that there is only one coil section for each magnet section, and the inner iron "stator" is actually part of the armature. The small size of this motor dictates these changes, but the small size also means that the side forces are relatively insignificant compared to those associated with the much larger piston motor.

The piston motor is required to provide real power output (equal to the thermodynamic load), with no reactive component. The gas compression and expansion in the Stirling cycle provides a gas spring for the piston mass, with the thermodynamic and dynamic parameters chosen so that the spring mass system is resonant at the cooler operating frequency. This results in the highest possible efficiency for the piston motor, since the motor does not have to accelerate the piston mass. See Reference 2 for a more detailed discussion of the refrigerator dynamics.

Conversely, the displacer is very nearly a purely reactive load. The motor force is actively used to accelerate and decelerate the displacer mass, while the damping load is fairly small, due only to the pressure drop

of the gas flowing through the regenerator and heat exchangers. The displacer motor, therefore, cannot be used in an efficient manner, since its power factor is near zero.

ANALYSIS

The electromagnetic force generated by a current flowing through a wire in a magnetic field is given by the relationship, F = B L I, where F is the force in Newtons, B is the magnetic flux density in Webers/m^2, L is the length of wire within the magnetic field in meters, and I is the current in Amperes. Estimating B, the magnetic flux density in the air gap occupied by the coil, is somewhat difficult. Magnetic materials are inherently non-linear, and the flux path of least resistance is not always apparent, since flux leakage is frequently significant. Philips Laboratories has available a proprietary finite-element computer package (MAGGY) which is designed specifically for the solution of magnetic problems. This program has been verified through extensive use by various Philips organizations, and is generally accurate to within a few percent. All calculations of magnetic performance, including estimates of motor inductance, were made using the MAGGY program. This allowed for the optimization of dimensions to obtain the maximum motor efficiency for a given motor weight, with the magnets operating at their peak energy product and the iron stator thickness minimized.

DESIGN PARAMETERS

Table II shows a comparison between the design values and the results measured during refrigerator operation for the piston and displacer motors. The refrigerator was producing 5 W at 65°K with a phase angle between piston and displacer motions of 60°. It should be noted that the force constant and losses in the displacer motor are substantially different than predicted. The effect of this on refrigerator performance is disussed in Section 7.

PISTON-MOTOR TEST DATA

As part of the effort to develop the linear motors, a task was undertaken to experimentally measure various characteristics of the piston motor. These included the electrical characteristics which affect the design of the control system and the mechanical characteristics which affect the design of the bearings supporting the piston.

The design of the fixture (see Fig. 15) can be divided into two major sections: the motor (on the left), and a gas spring (on the right). There is also a means for attaching the two and a rigid system to keep the apparatus aligned.

The motor, consisting of the stator (22) and the armature (23), is, of course, the motor to be tested. The armature is attached to a linear air bearing (25) which in turn is attached, through a force transducer (28), to the gas-spring mechanism. An air bearing was used for its low power dissipation, accurate location, and light-weight construction.

The gas spring consists of a cylinder (15) and a two-sided piston (16). The cylinder is pressurized so that in moving the piston, a considerable force is required to compress the gas, yielding its spring-like characteristic. This gas spring was designed so that its nonlinearities, inherent to all gas springs, would be comparable to those found in the cooler, thus producing a representative environment for testing.

Rulon sleeves were used on the piston as a combination clearance seal and bearing. The low coefficient of friction of Rulon assured low power dissipation, and a 8 μm radial gap produced an acceptable clearance seal.

A system of valves is used to change the mean pressure within the cylinder, which changes the stiffness of the gas spring and thus the dynamic resonant frequency of the motor fixture. The valve system can also dissipate energy by allowing gas to flow between the cylinder halves. By controlling this flow, any desired motor loading can be produced.

Incorporated into the fixture design are three piezoelectric force transducers and an LVDT. The two radial force transducers located at the ends of the shaft (27) measure the side forces which the magnetic bearings will encounter. The third force transducer (28), mounted between the armature and the spring mechanism, measures the axial force and torque. The LVDT (20, 18) is mounted inside the cylinder and measures the position of the oscillating system at any time. A photograph of the motor test fixture is shown in Figure 16.

Measurements taken with this fixture are summarized below.

Force Constant. The axial force constant was predicted to be 8.8 N/Amp, using the MAGGY computer program. The measured dc value, representing the average of 16 measurements, was 8.77 N/Amp $\pm$ 0.24 N/Amp standard deviation.

Efficiency. Motor efficiency was measured for a wide range of force output and stroke amplitude. In all cases, the measured efficiency was within 10% of the predicted value.

Temperature Rise. The average temperature of the motor coil during operation was obtained by measuring its resistance (since the resistivity of copper is a known function of temperature). Measurements showed a temperature rise of about one-half of a degree centigrade per watt of power dissipation in the coils, giving a coil temperature of 35°C at the design point.

Side Forces. The force transducer measurements indicated that the static side forces (due to magnetic assymetries) were less than 10 N on all axes,

and the dynamic side forces (due to coil and/or mechanical assymetry) were less than 5 N. This is well within the measured capability of the magnetic bearings.

Torque Generation. Although the motor is linear, it will generate some torque due to the same assymetries responsible for the side forces. The torque was somewhat difficult to measure, but a conservative upper bound was 5 N-m at 25 Hz. Given the large moment of inertia of the piston assembly, this level of torque would result in a torsional oscillation of only 1° peak rotation.

CONCLUSIONS

The design procedures described here have resulted in the successful development of linear motors which met all requirements of the current refrigerator program. Analytical and numerical performance-prediction techniques were validated to a high degree of accuracy.

AXIAL CONTROL SYSTEMS

GENERAL

The axial control loops of the piston and displacer motors are intended to ensure long-term, stable refrigerator operation and to minimize harmonic vibrations. In order to achieve this stability the control loop errors of amplitude, phase and center position had to be minimized over a wide frequency range. The control loop can be broken down into three major sections: axial position transducer (LVDT), motor driver, and compensation.

AXIAL POSITION TRANSDUCER

The position transducers used in the refrigerator are a slightly modified version of a commercially available transducer. The LVDT produces an electrical output proportional to the displacement of a non-contacting ferromagnetic core. The motion of the core varies the mutual inductance of the differential secondary windings of the transformer. In addition to the ac excitation of the primary, synchronous demodulation and filtering of the transformer output is needed to extract the position signal. Improvements to the commercial transducer system involved improving the frequency stability of the ac excitation.

MOTOR DRIVER

The piston and displacer motor drivers are linear amplifiers with a deliverable power capability in excess of 300 Watts RMS. The amplifiers were designed with a bridge output configuration in order to effectively increase the applied motor voltage capability above the 28 V power supply. This additional voltage "headroom" compensates for motor parameters which

change as a function of operating frequency. The disadvantage of the bridge configuration is that the load is in effect "floating" above ground, which makes closed-loop current control difficult. Further, the maximum efficiency of the amplifier is reduced by a factor of two because of the additional power transistor in series with the load.

In order to analyze the amplifier performance and provide stability to the closed loop current control the effective motor impedances, a function of the motor load, are required. To estimate these impedances, the equivalent circuits for the piston and displacer motor systems (see Fig. 17 and 18), which are a linear approximation of the refrigerator dynamics at the operating point, are derived. In the case of the piston, the motor will operate at or near mechanical resonance (power factor of 1). This is achieved as a result of the balance between the inertial force of the piston and the spring force of the gas. The mechanical/electrical analog is simplified by modeling the linear motor as an ideal transformer (using SI units). Therefore the reflected inductance and capacitance, at the primary of the transformer, will be in resonance and have an infinite impedance. The mechanical damper, when reflected, represents the dynamic motor load which is in series with the piston motor coil.

Since the displacer assembly was not designed to operate in resonance (there is no spring), the effective impedance at the operating point is a function of the displacer mass and the coupling of the piston force through the gas. The dynamic load of the displacer is primarily reactive and the net power delivered to the thermodynamics (excluding ohmic losses) is very small, on the order of a few watts. The effect of the mass is also small, and thus the equivalent circuit of the displacer motor and load is simply the motor coil impedance.

The equivalent circuits of the piston and displacer motors are used to determine the peak currents and voltages required at the operating point. Once the output requirements were defined, the driver and input stages were designed to meet specific amplifier operating requirements of stability and bandwidth. For both drivers a peak current of 25 amps at the operating frequency was specified with less than 1% gain sensitivity to internal component variations. The full power bandwidth of both current drivers is designed to be greater than 1.5 kHz.

COMPENSATOR

A general block diagram of the piston and displacer axial control loops is shown in Figure 19. The gain and frequency response of the position transducers and current amplifiers are determined. The compensator is designed to optimize the position loop response. The two major objectives for the control loops are to minimize the sensitivity of the system to internal changes in the dynamics and to achieve a phase margin of at least 40° for stability. The finite bandwidths of the amplifiers and position transducers, and the vibrational resonances of the piston and displacer

shafts are considered in the calculation of the achievable system frequency response. The final piston and displacer control loops resulted in less than 10% gain sensitivity to system changes at the operating frequency and a phase margin of 50° with bandwidths of 65 Hz and 105 Hz, respectively.

COUNTERBALANCING SYSTEM

DESCRIPTION

Axial vibrations induced by the motions of the piston and displacer are attenuated by a passive vibration absorber. This device, shown schematically in Figure 20, consists of a 3.0 kg mass suspended at its ends by leaf springs. This type of suspension was chosen to minimize damping and to provide radial centering accuracy. The mass is also attached to a stiff coil spring on which it resonates at the cooler operating frequency. The stroke amplitude is 5.0 mm.

After a short period of refrigerator operation, it was observed that small movements between the coil spring and its mount were causing the generation of particles by a process called fretting. This problem has been temporarily reduced by clamping the spring to the mount, but a permanent solution is needed. Although there is always a potential problem when moving parts have mechanical contact, relatively long life is still a possibility. Further, since the countermass housing is distinct from the working space of the refrigerator, lubrication is possible.

PREDICTED PERFORMANCE

To predict the performance of the balancer, a linear two degree of freedom vibration model is used (see Fig. 21). The mass of the balancer is connected by a damped spring to the refrigerator housing, which is in turn connected through a damped spring to inertial ground. Figure 22 is a plot of the predicted force transmission as a function of cooler frequency. In this case, maximum attenuation occurs at 26 Hz. The sharpness of the attenuation is a result of the low damping in the coil spring and the leaf spring mount of the countermass. If the refrigerator is run at frequencies other than 26 Hz, the transmitted force sharply increases. At 26.5 Hz, a natural frequency of the two degree of freedom system, the vibration is amplified because the countermass reciprocates in phase with the refrigerator piston and displacer. A second natural frequency, related to the resonance of the mount, is low enough to be of no concern. Note that the vibration absorber will remove only the fundamental frequency. Higher harmonics will not be attenuated significantly.

The 63 Kg refrigerator is mounted to the table through coiled-wire springs (see Fig. 2) and exhibits a measured natural frequency of 6 Hz with a damping factor, ζ_M of 0.07. Measurements taken on the countermass coil spring indicated a desirably low damping factor of only .0014. Using these

values a vibration attenuation of 22 dB is the calculated additional effect of the balancer.

PERFORMANCE DATA

An accelerometer was first mounted to the cooler without the countermass installed. Test data was obtained using a piston amplitude of 7.3 mm and a displacer amplitude of 3.0 mm with a phase shift of 67° at 26 Hz. Next, the countermass system was installed and the accelerometer data was retaken.

It can be seen in Table III that the agreement between actual and predicted performance is good. As a point of comparison, the piston and displacer masses exert a peak disturbance force (inertial) of 415 N. Thus, the counterbalancing system only transmits 0.3% of this force at the fundamental frequency. The small cooler motion and low force transmittal to the base is accomplished without the use of additional electrical input power.

REFRIGERATOR PERFORMANCE

The refrigerator was successfully operated beginning in March 1982. The cooldown curve (temperature vs. time) is given in Figure 23. Table IV shows a comparison between the predicted performance, calculated with the Philips Stirling Analysis Computer Program, and that actually measured. The lower operating frequency is used because the piston mass is higher than predicted. The charge pressure, which determines the gas spring stiffness, could also be raised to keep the system in resonance. The countermass was tuned to resonate at 25 Hz for operation with the refrigerator.

The discrepancy in the electrical input power to the motors can be explained in two ways. First, the measured power includes higher harmonics of the running frequency. The dissipation of power at these frequencies results from the action of the axial control system and is not included in the Stirling program.

Secondly, as noted in Section 4, the electrical input power to the displacer motor, at the fundamental frequency, is substantially higher than predicted. The measured dynamic force constant was lower than predicted, necessitating the use of higher input currents to generate the required force. The flux density of the Permendur in the motor armature was designed to be very close to magnetic saturation, with a magnitude as high as 2.4 Tesla. At this level of flux density, the uniformity of the material becomes critical, as does the manner in which it is annealed. Since the diameter of this motor was restricted by the small size of the displacer, no margin was available for a conservative design.

A resistive heater is used to apply the load power at the cold end of the refrigerator. Figure 24 shows the parametric effect on cold temper-

ature and input power of varying this heater load. For this test, the amplitude and phase of the moving elements, along with the operating frequency, were held fixed. The input power decreases with increased load since the Carnot efficiency increases with the higher temperature.

Figure 25 shows the effects of varying the phase shift between the piston and displacer motions while holding amplitudes and frequency fixed. For this test, the temperature was held constant by adjusting the load power of the heater.

FUTURE PLANS

Philips Laboratories is currently under contract with NASA-Goddard Space Flight Center to produce the second generation of this magnetically suspended refrigerator. Efforts will be directed at reducing electrical input power and at meeting flight qualification requirements. Additional attention will be given to the overall system interactions. The first step in the development is a parametric characterization of the present model, of which Figures 24 and 25 represent the first two tests.

REFERENCE

1. Philips Laboratories, Division of North American Philips Corp., Design and Fabrication of a Long-Life Stirling Cycle Cooler for Space Applications, Phase I and II - Engineering Model, Final Report: Sept. 1978 - Dec. 1982, by F. Stolfi, M. Goldowsky, C. Keung, L. Knox, E. Lindale, R. Maresca, J. Ricciardelli, P. Shapiro, NASA contract NAS5-25172, Briarcliff Manor, N.Y., March 1983.

2. A.K. de Jonge: A Small Free-Piston Stirling Refrigerator. The Fourteenth Intersociety Energy Conversion Engineering Conference, Boston, Mass, August 1979.

TABLE I.--MAGNETIC BEARING PERFORMANCE.

	Piston	Displacer
D.c. Offset (Due to Shaft Weight)	<.4 μm	<.5 μm
Peak a.c. Oscillations (During Operation)	<.7 μm	<2.5 μm
Control Loop Bandwidth	375 Hz	150 Hz
Control Loop Phase Margin	40°	40°
Calculated d.c. Stiffness	26 x 10^6 N/m (150,000 lbs/in)	5.3 x 10^6 N/m (30,000 lbs/in)
Worst Case Sensor Drift Observed While Operating	.25 μm	.75 μm
Wideband Sensor Noise Level	~.25 μm	~.25 μm

TABLE II. --MOTOR PARAMETERS.

Parameter	Piston Motor		Displacer Motor	
	Design	Measured	Design	Measured
Peak force (N)	150	189	35	37
Phase angle of force from displacement (°)	90	90	176	180
Operating frequency (Hz)	26.7	26.7	26.7	26.7
Stroke amplitude (mm)	7.0	7.0	3.0	3.0
Force constant (N/A)	8.8	8.8	5.0	3.7
Real power output (W)	88	110	0.6	
Peak applied voltage	15	16	12	18
Peak current (A)	17	22	7	10
Ohmic Loss (W)	29	46	40	91
Efficiency (%)	75	71	N/A	N/A

TABLE III.--COUNTERMASS TEST RESULTS.

	Fundamental (26 Hz)	2nd. Harmonic (52 Hz)	3rd. Harmonic (78 Hz)
Without Balance:			
Peak acceleration (m/sec^2)	6.6	0.51	0.11
Peak displacement (μm)	252.	19.3	4.1
Peak transmitted force (N)	24.	1.9	0.4
With Balance:			
Peak acceleration (m/sec^2)	0.35	0.44	0.14
Peak displacement (μm)	13.4	16.8	5.3
Peak transmitted force (N)	1.3	1.6	0.5

TABLE IV.--DESIGN VERSUS PERFORMANCE.

Quantity	Design Value	Measured Value
Piston moving mass (kg)	1.85	1.92
Displacer moving mass (kg)	0.32	0.35
Piston amplitude (mm)	7	7.3
Displacer amplitude (mm)	3	3.0
Phase between piston and displacer (deg)	60	67
Operating frequency (Hz)	26.7	25.0
Charge pressure (atm)	16	16
Ambient heat exchanger temperature (°C)	15	12
Electric input power to motors (W)	155	220
Cold production (W)	5	5
Cold temperature (°K)	65	64.6

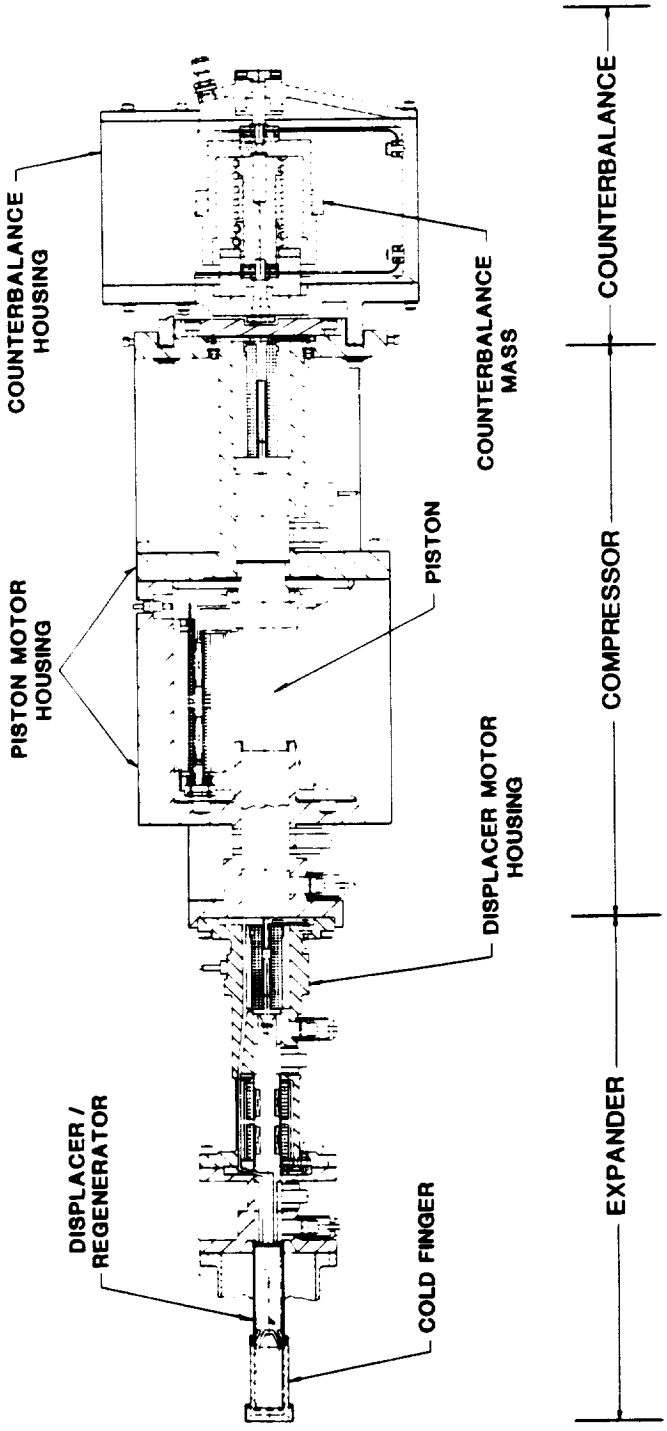

Figure 1. Cross-sectional view of refrigerator.

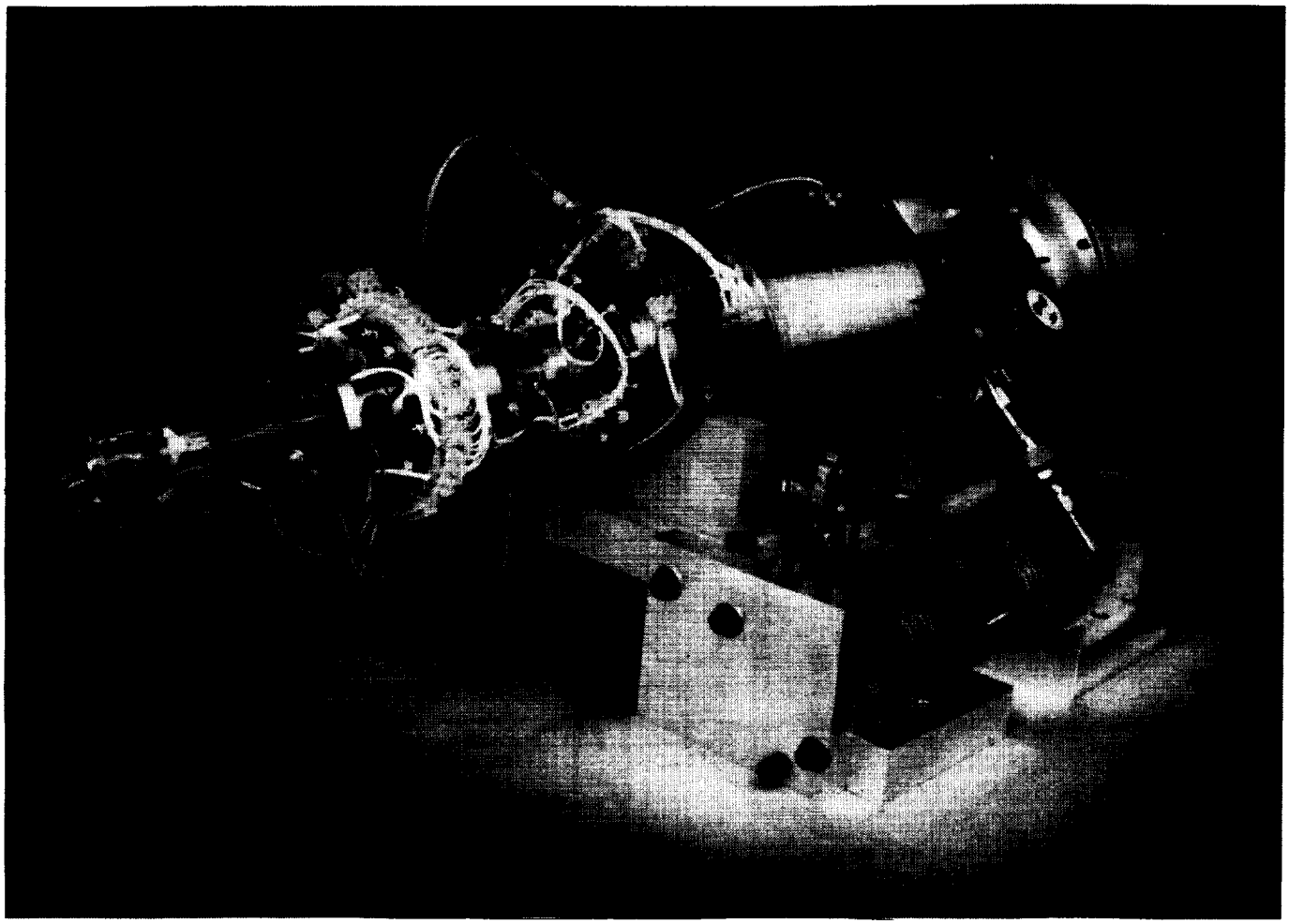

Figure 2. Cryogenic refrigerator.

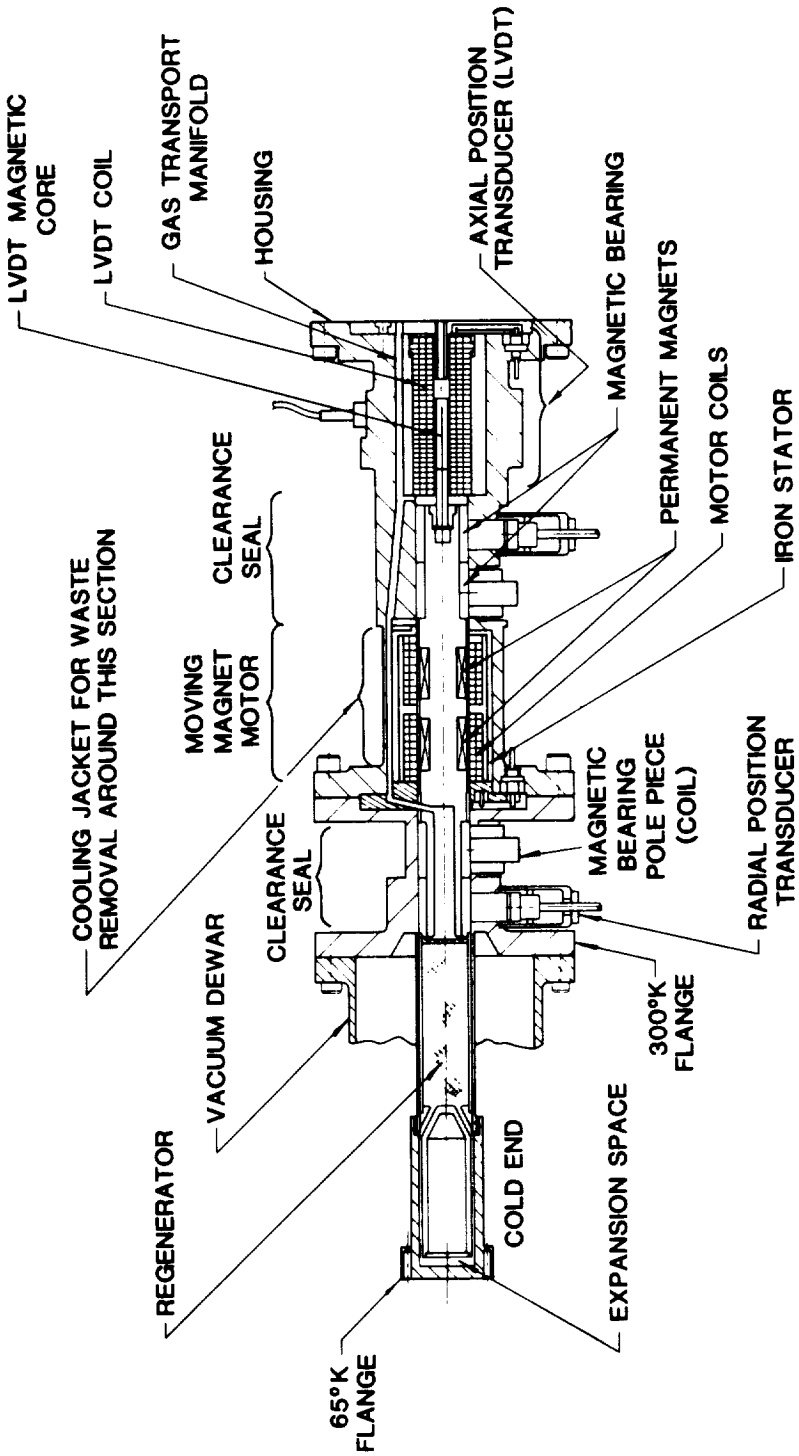

Figure 3. Displacer subassembly.

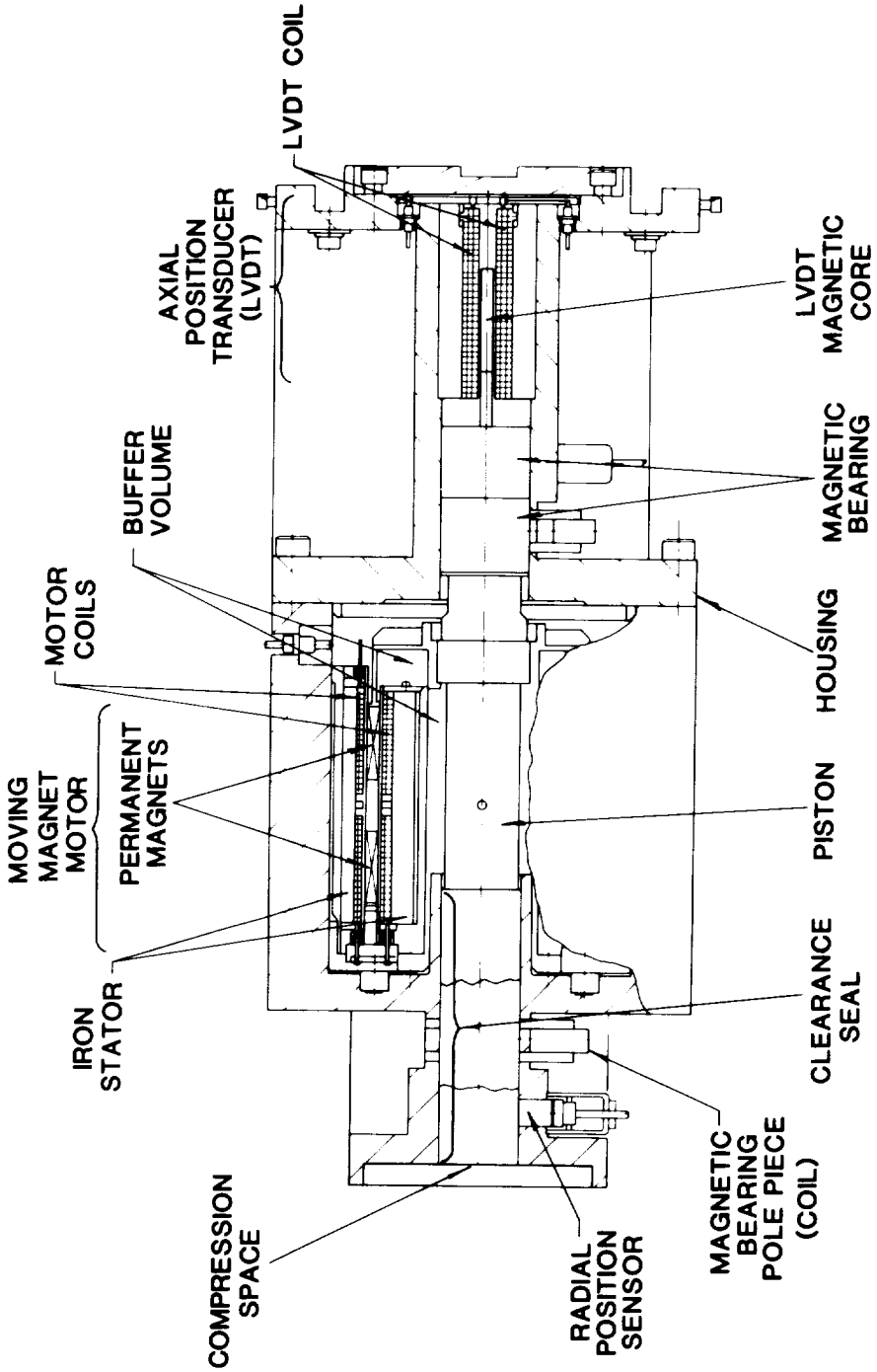

Figure 4. Piston subassemmly.

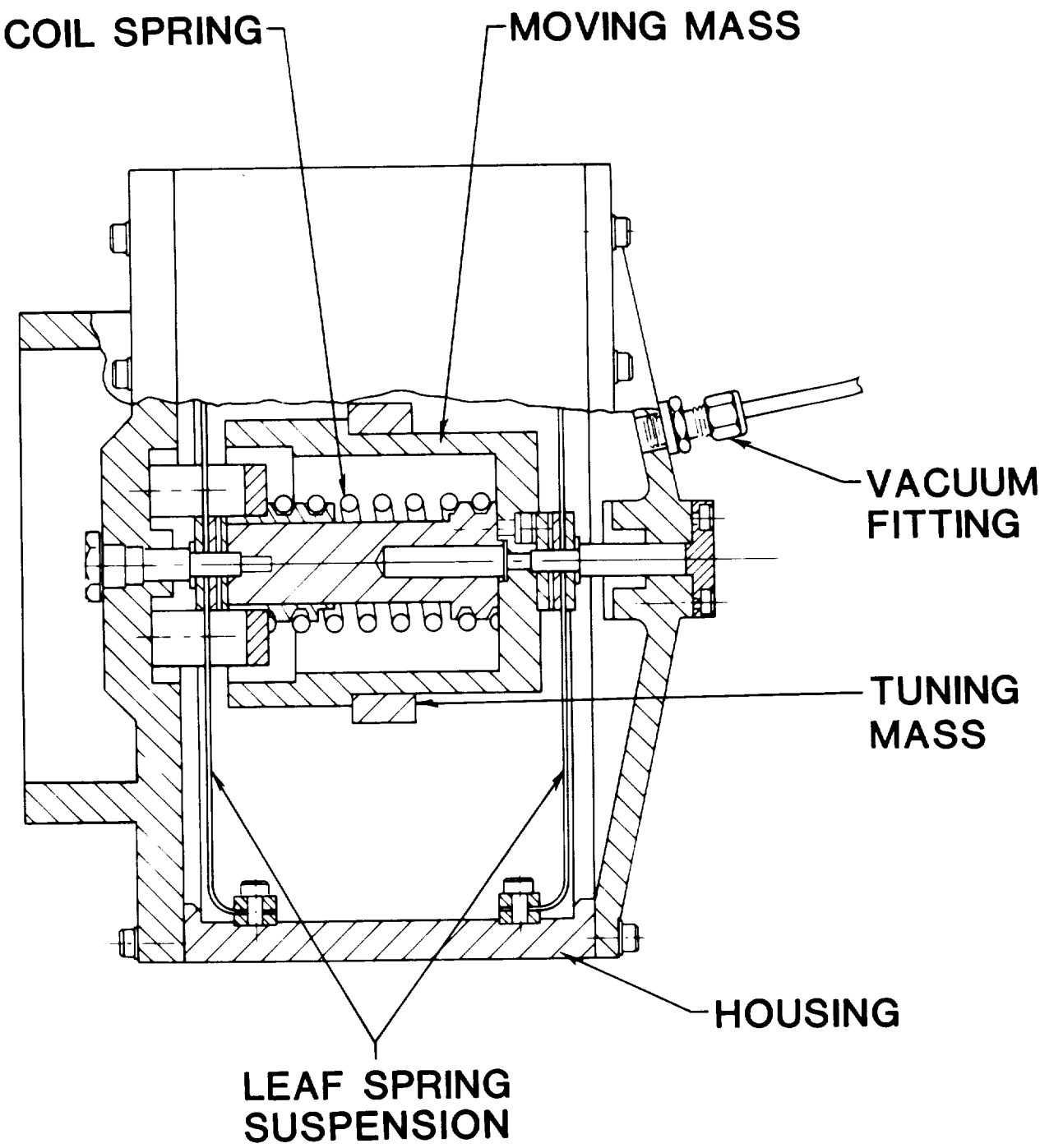

Figure 5. Countermass subassembly.

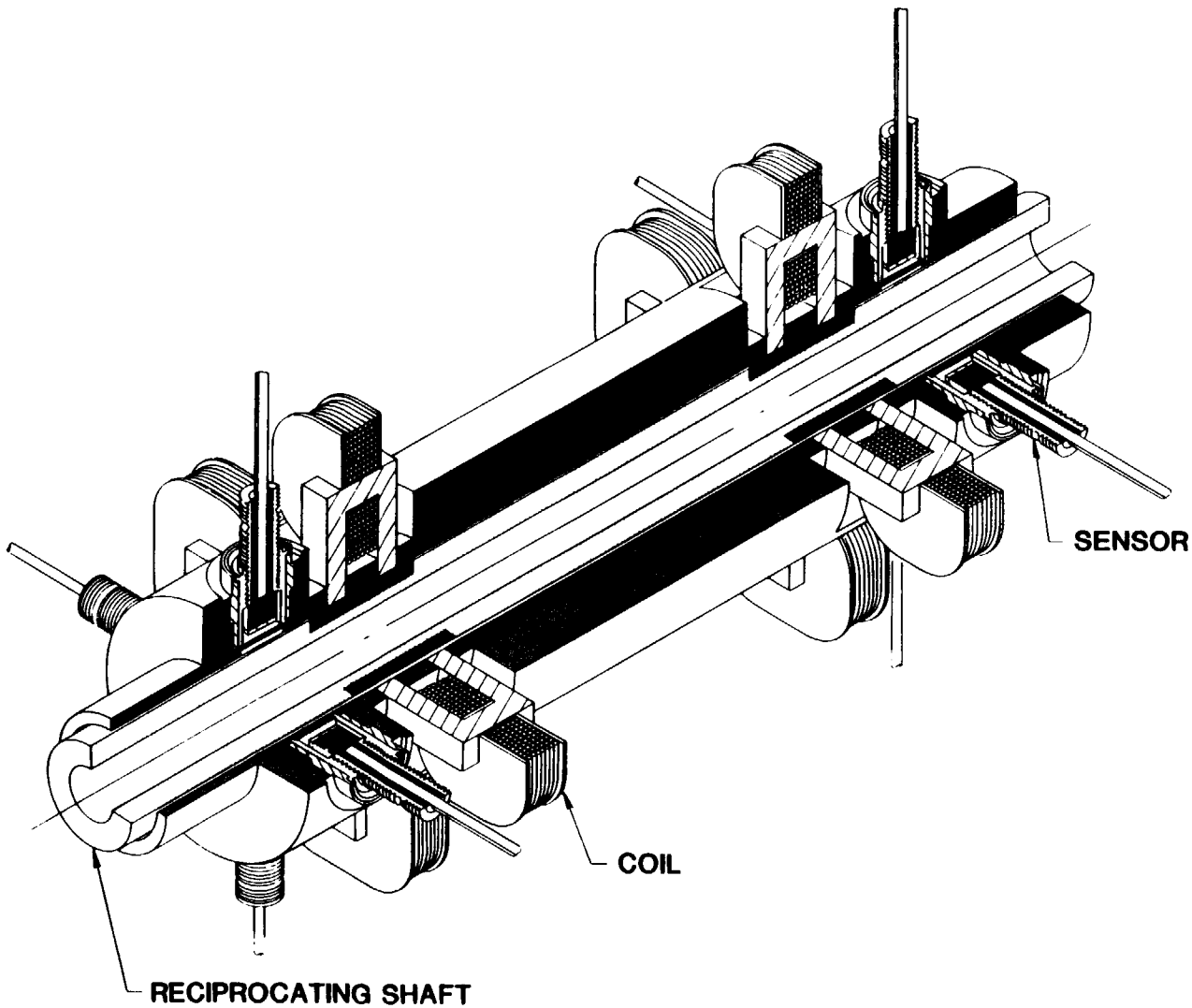

Figure 6. Schematic of magnetic bearing.

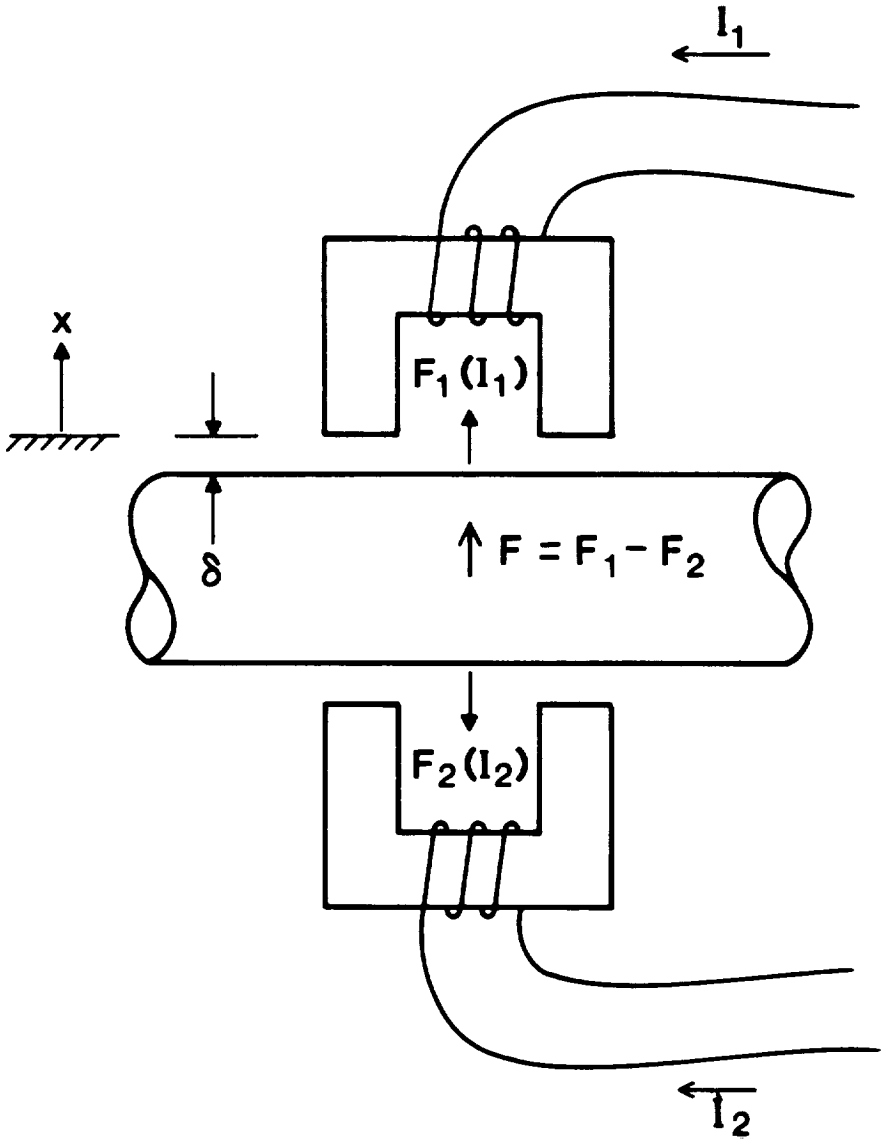

Figure 7. Radial force generation in magnetic bearing plane.

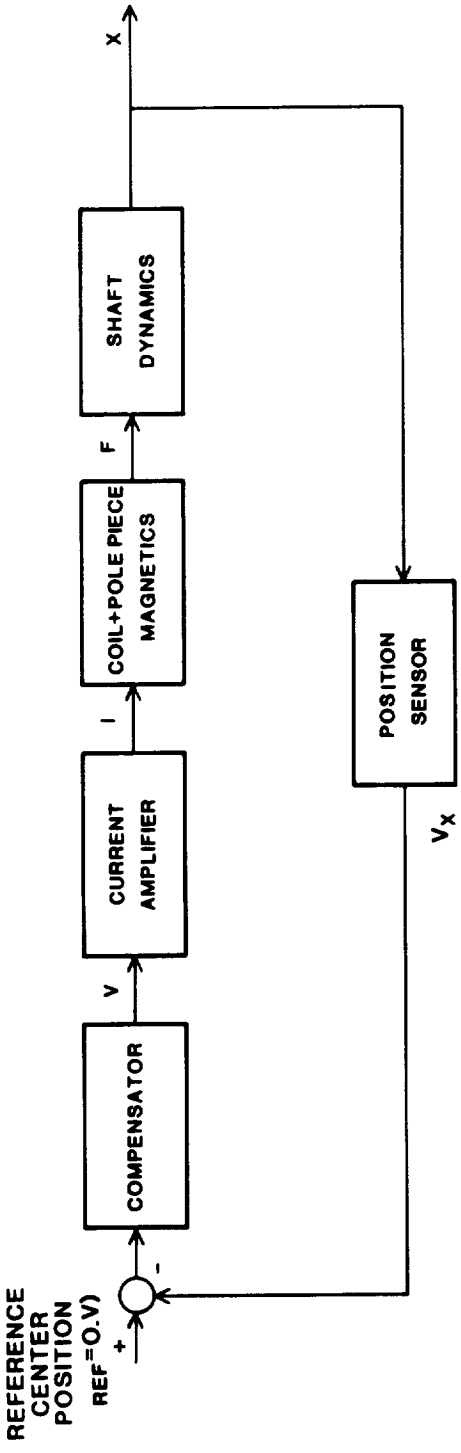

Figure 8. Bearing control sysytem block diagram.

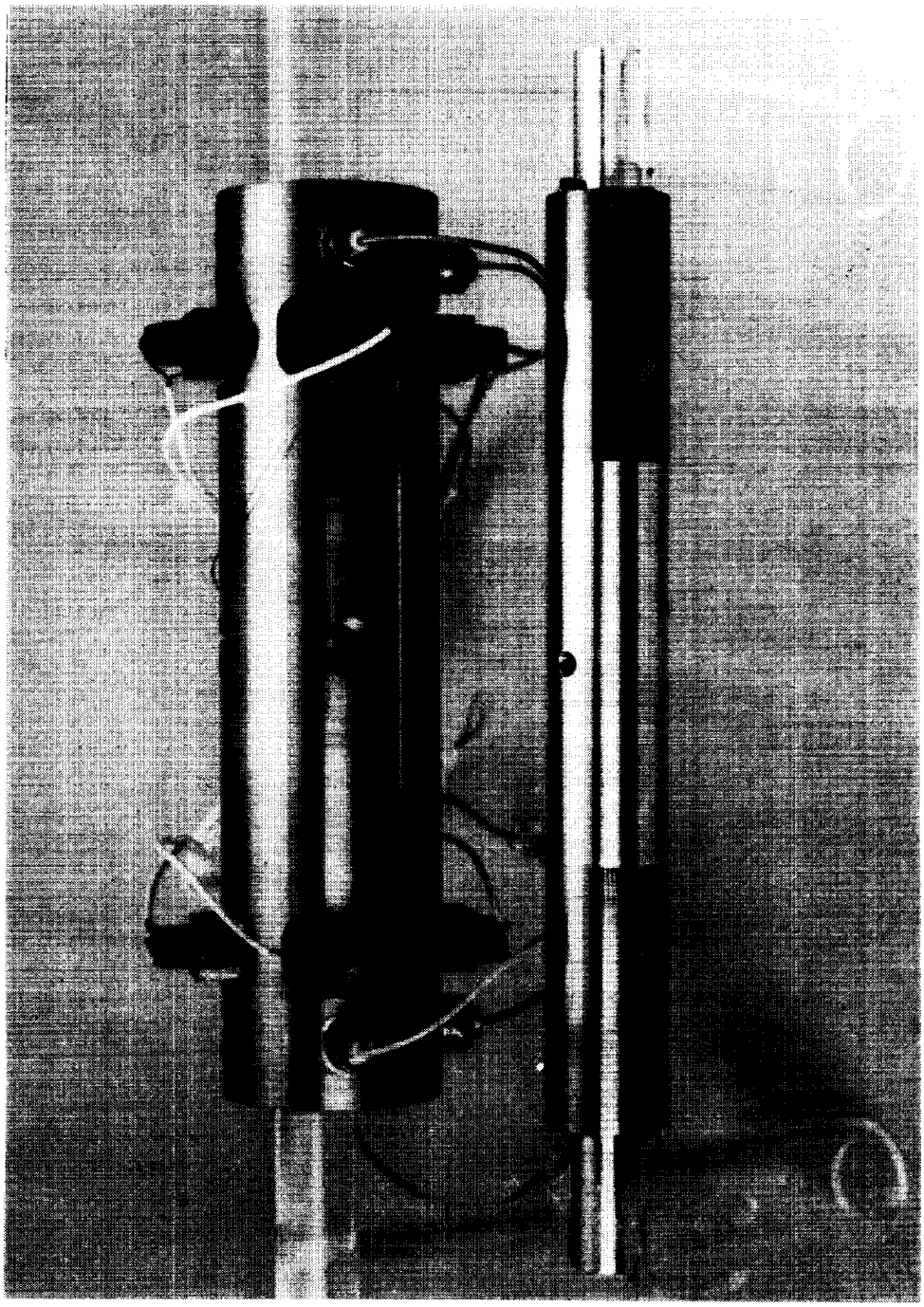

Figure 9a. Test fixture.

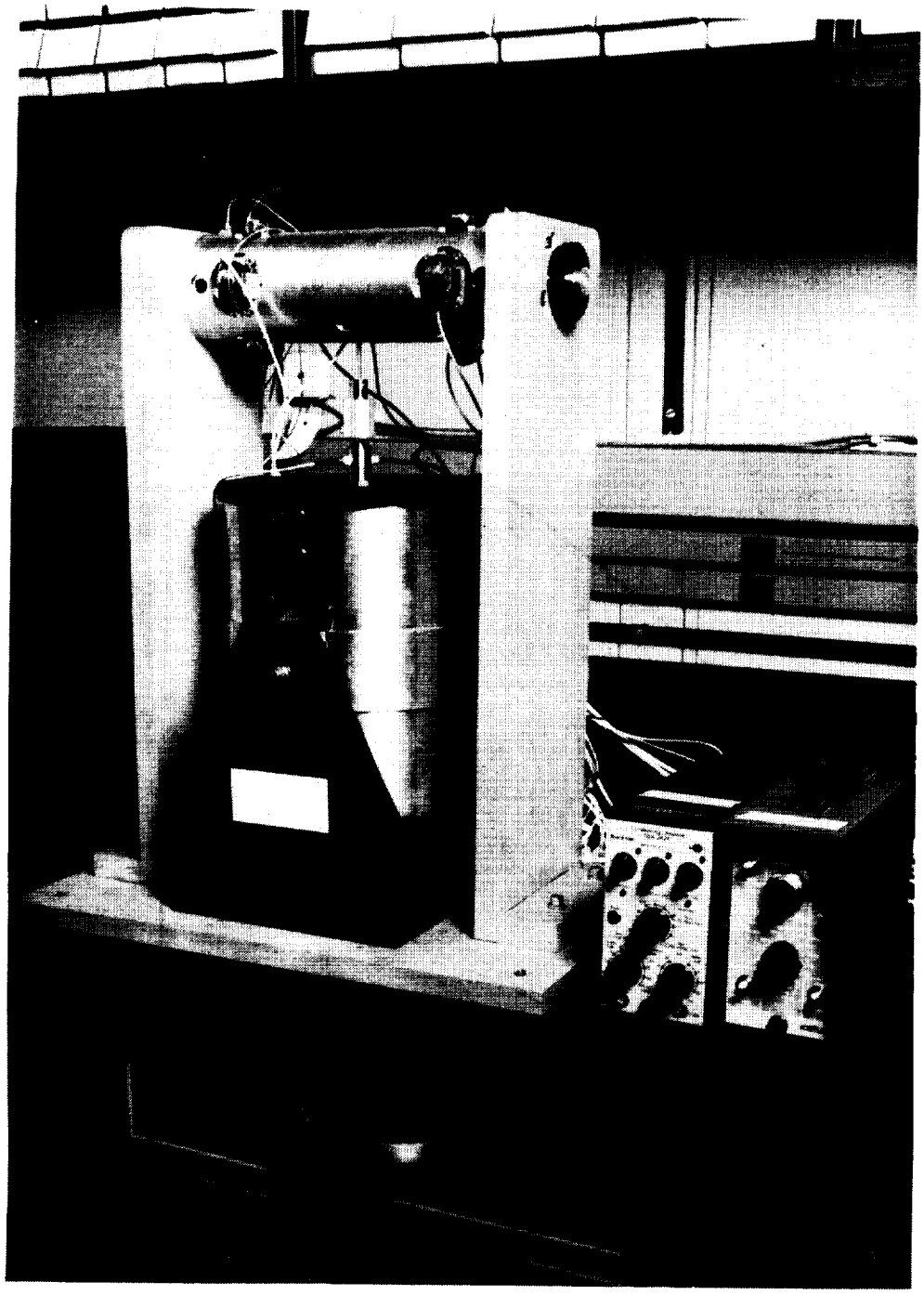

Figure 9b. Fixture on test stand.

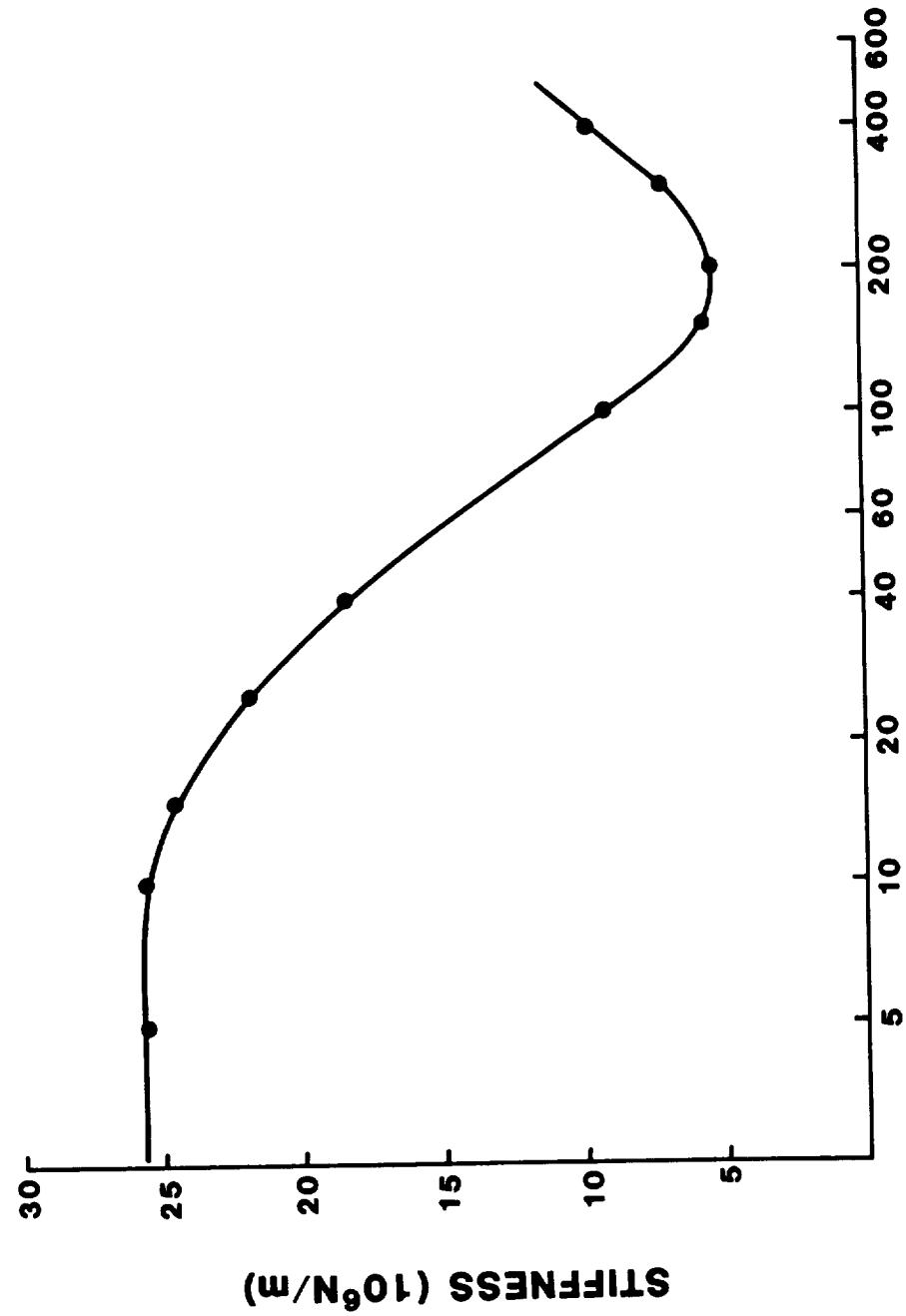

Figure 10. Magnetic bearing ac "stiffness".

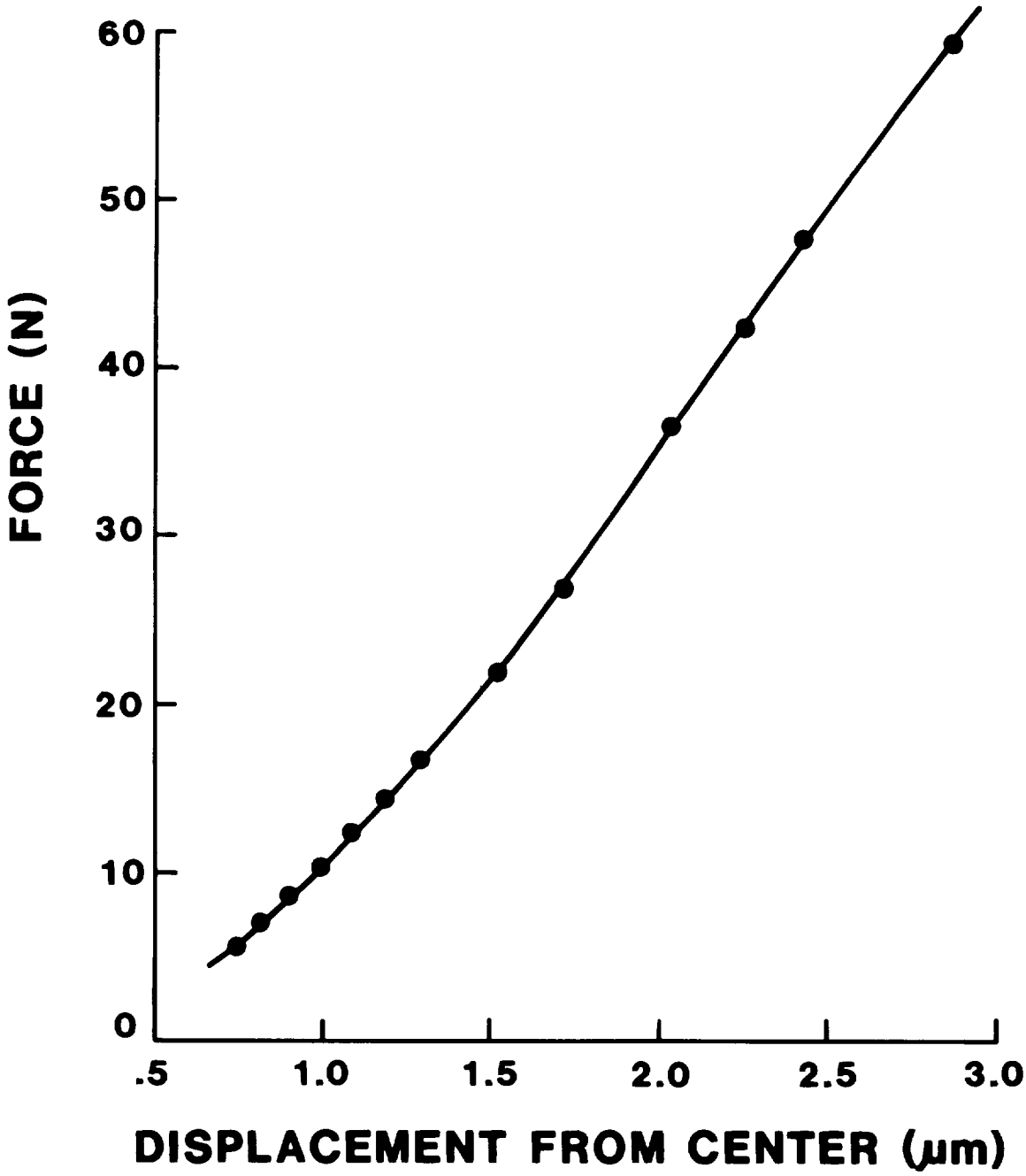

Figure 11. Magnetic bearing static load characteristics.

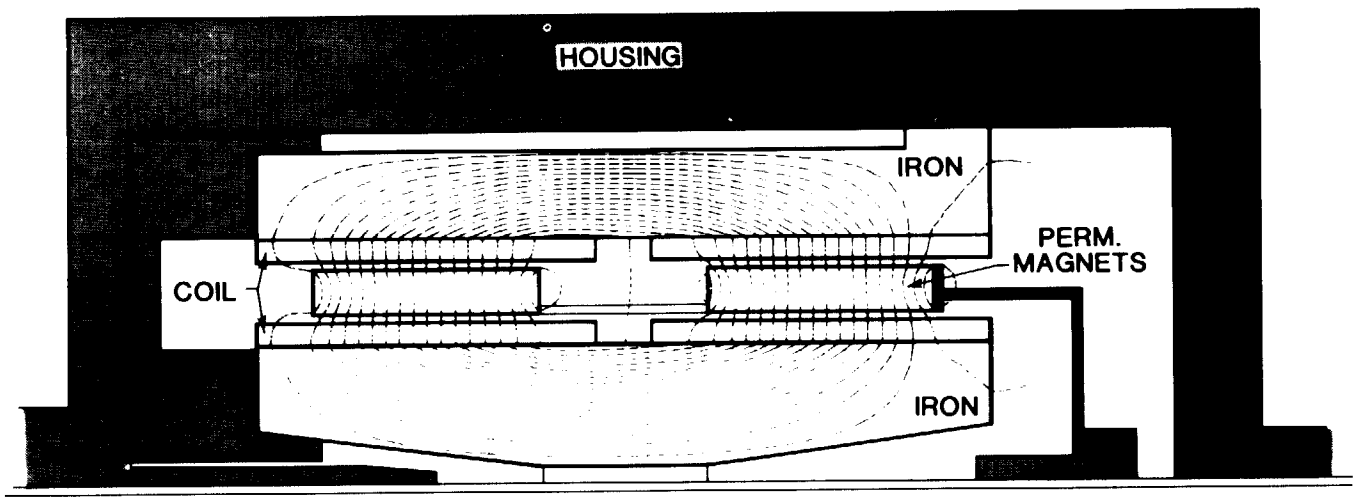

Figure 12. Schematic of linear motor for piston, showing lines of magnetic flux (armature in centered position).

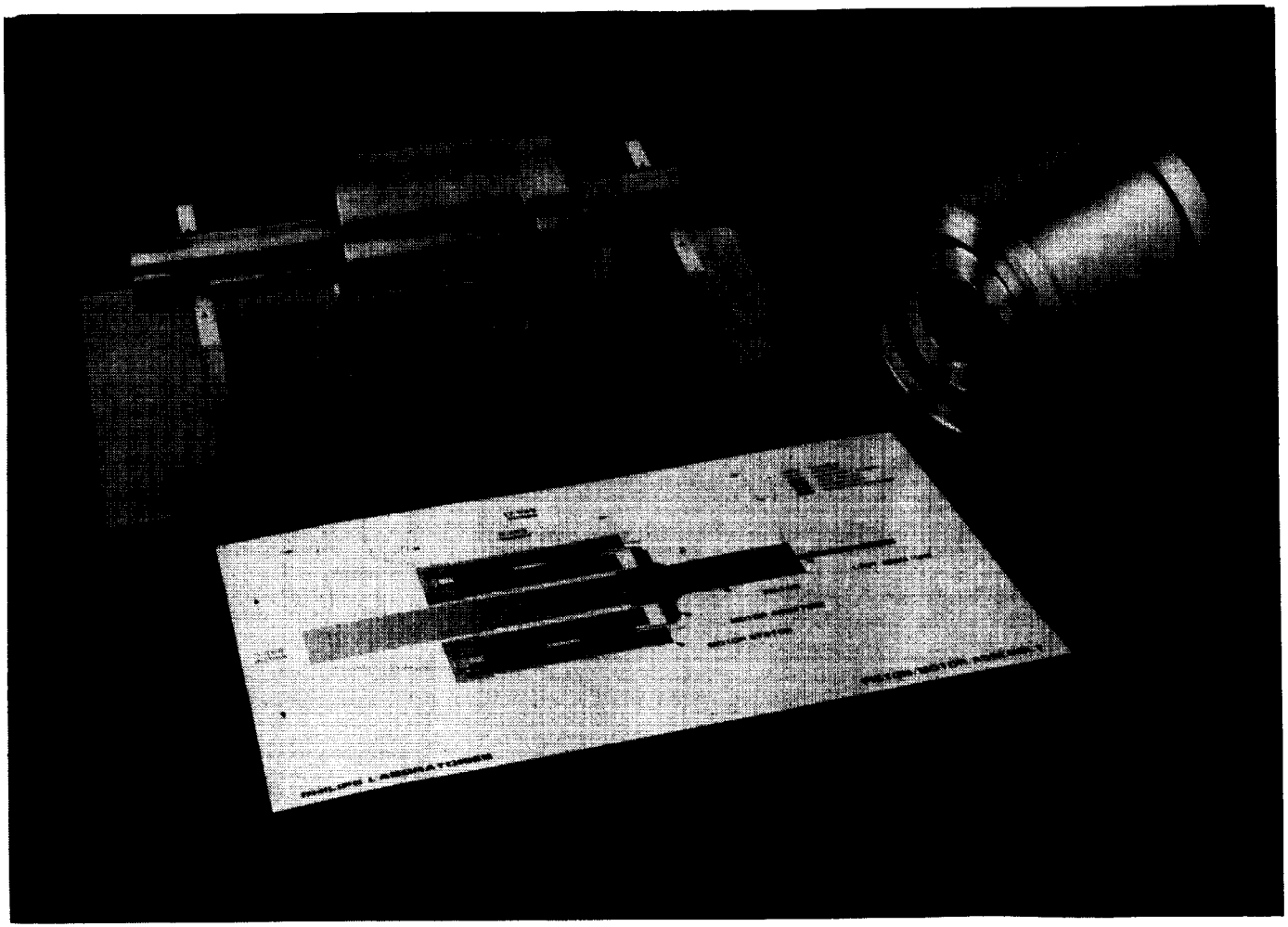

Figure 13. Completed piston armature on piston shaft, shown with stator assembly.

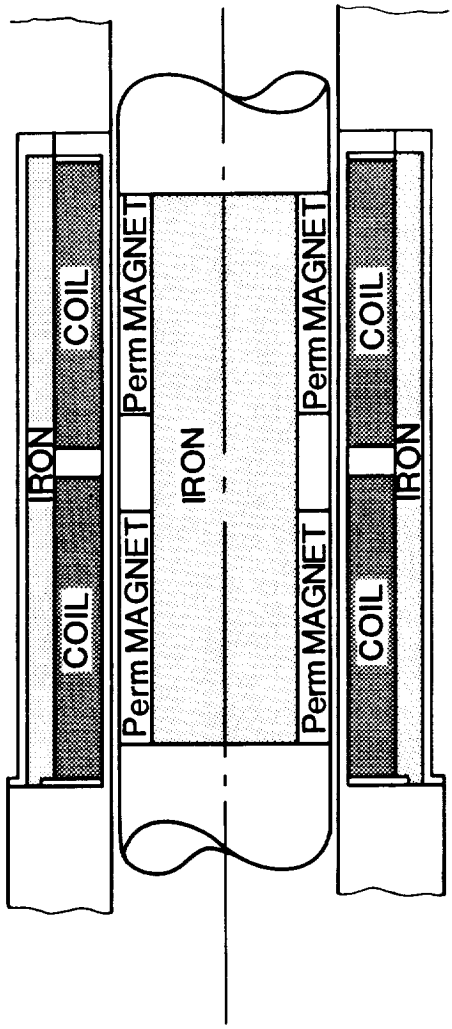

Figure 14. Schematic of linear motor for displacer.

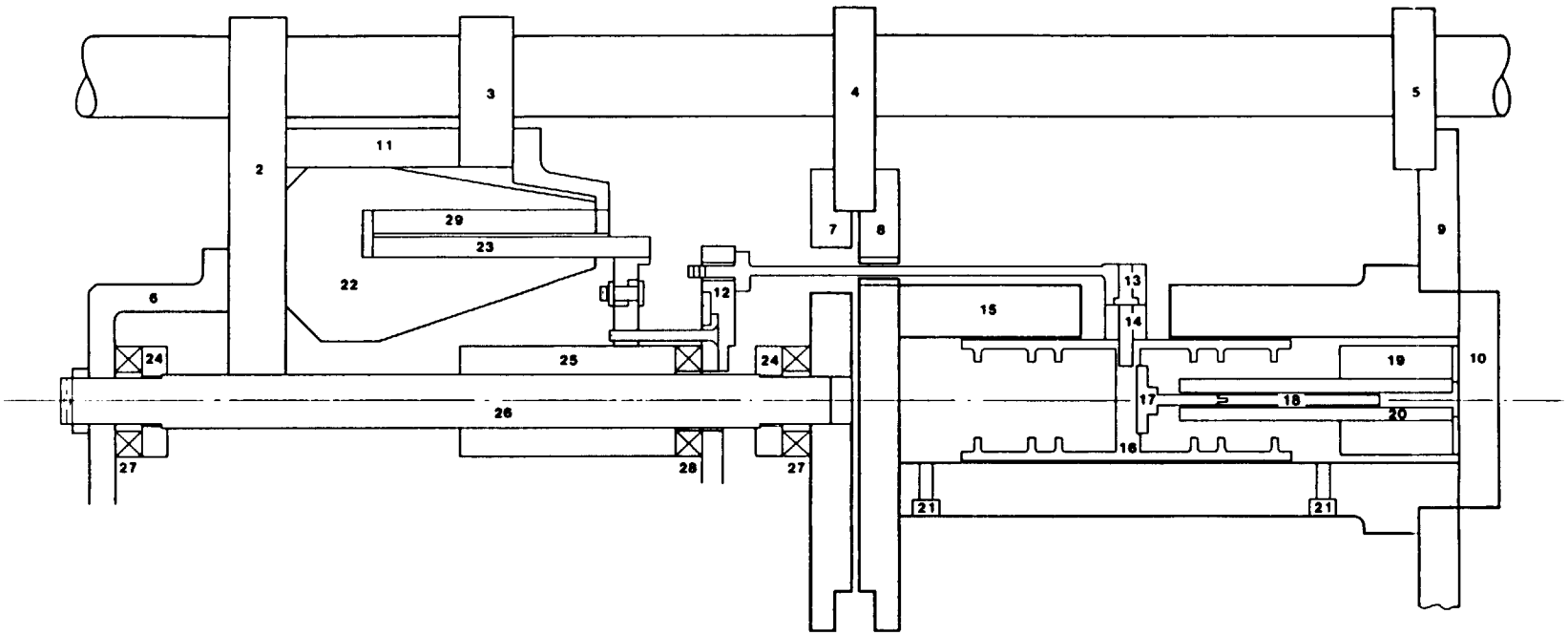

1) ALIGNMENT RODS (3)
2) MOUNTING PLATE
3) MOUNTING PLATE
4) MOUNTING PLATE, GAS SPRING
5) MOUNTING PLATE, GAS SPRING
6) MOUNTING PLATE
7) MOUNTING PLATE, GAS SPRING
8) MOUNTING PLATE, GAS SPRING
9) MOUNTING PLATE, GAS SPRING
10) END CAP
11) STATOR MOUNTING RING
12) SLIP RING LINKAGE
13) RODS (3)
14) ROD BUSHINGS (3)
15) GAS SPRING CYLINDER
16) PISTON
17) LVDT CORE SUPPORT
18) LVDT CORE
19) LVDT BODY HOLDER
20) LVDT BODY
21) PORTS (6)
22) STATOR
23) ARMATURE
24) F.T. CONNECTOR
25) BEARING
26) SHAFT
27) X-Y FORCE TRANSDUCER (2)
28) TORQUE-COMPRESSION F.T.
29) MAGNET ASSEMBLY

Figure 15. Schematic of piston-motor test fixture.

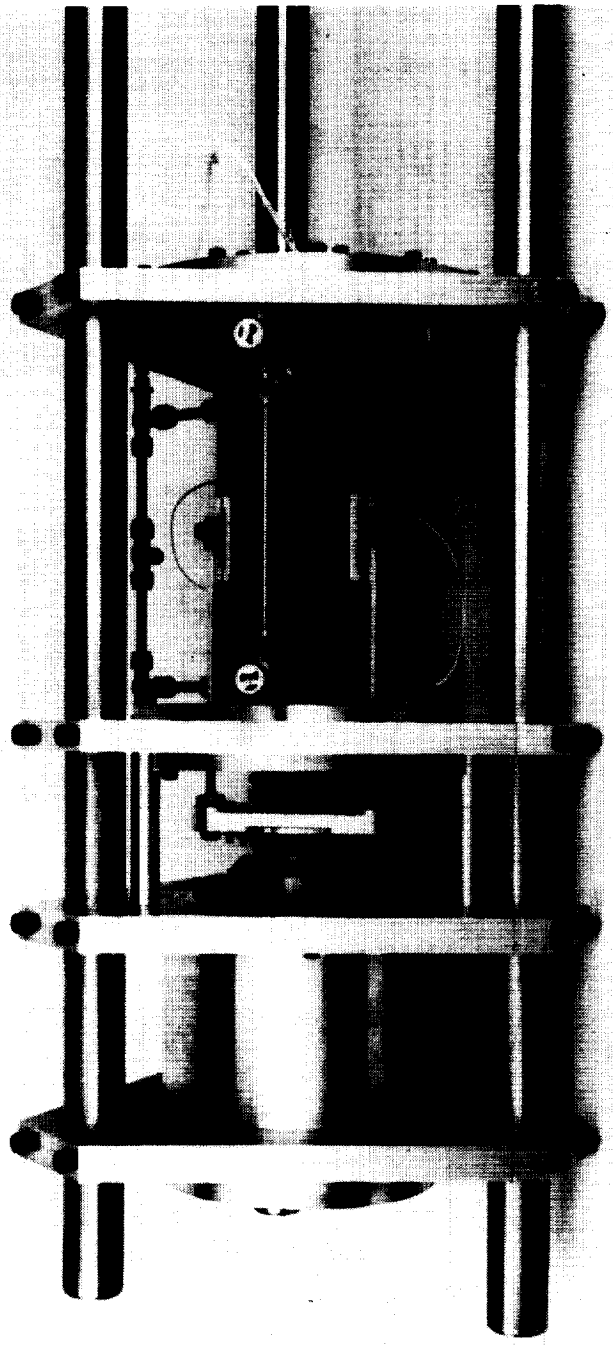

Figure 16. Piston-motor test fixture.

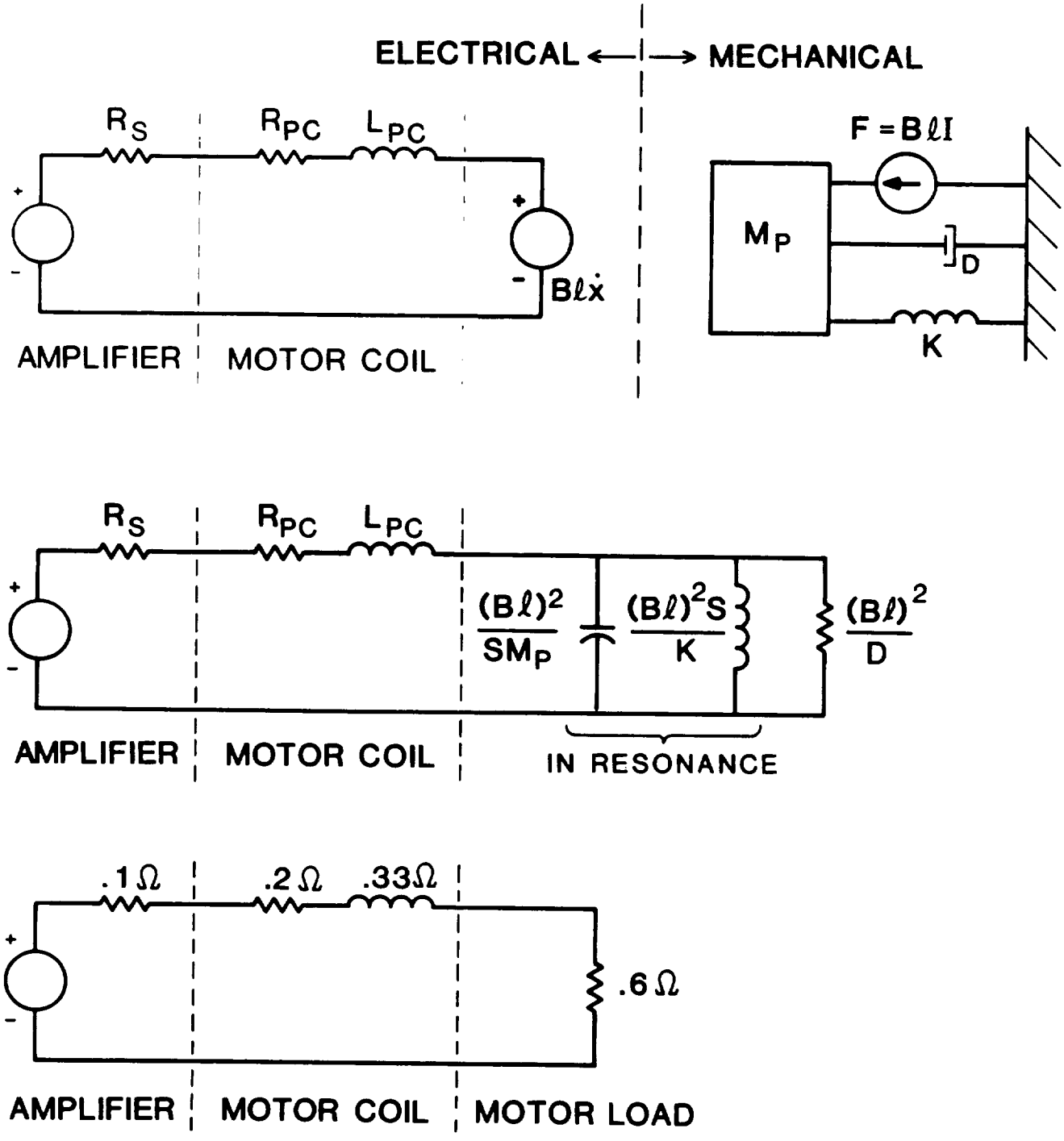

Figure 17. Derivation of effective piston system impedance.

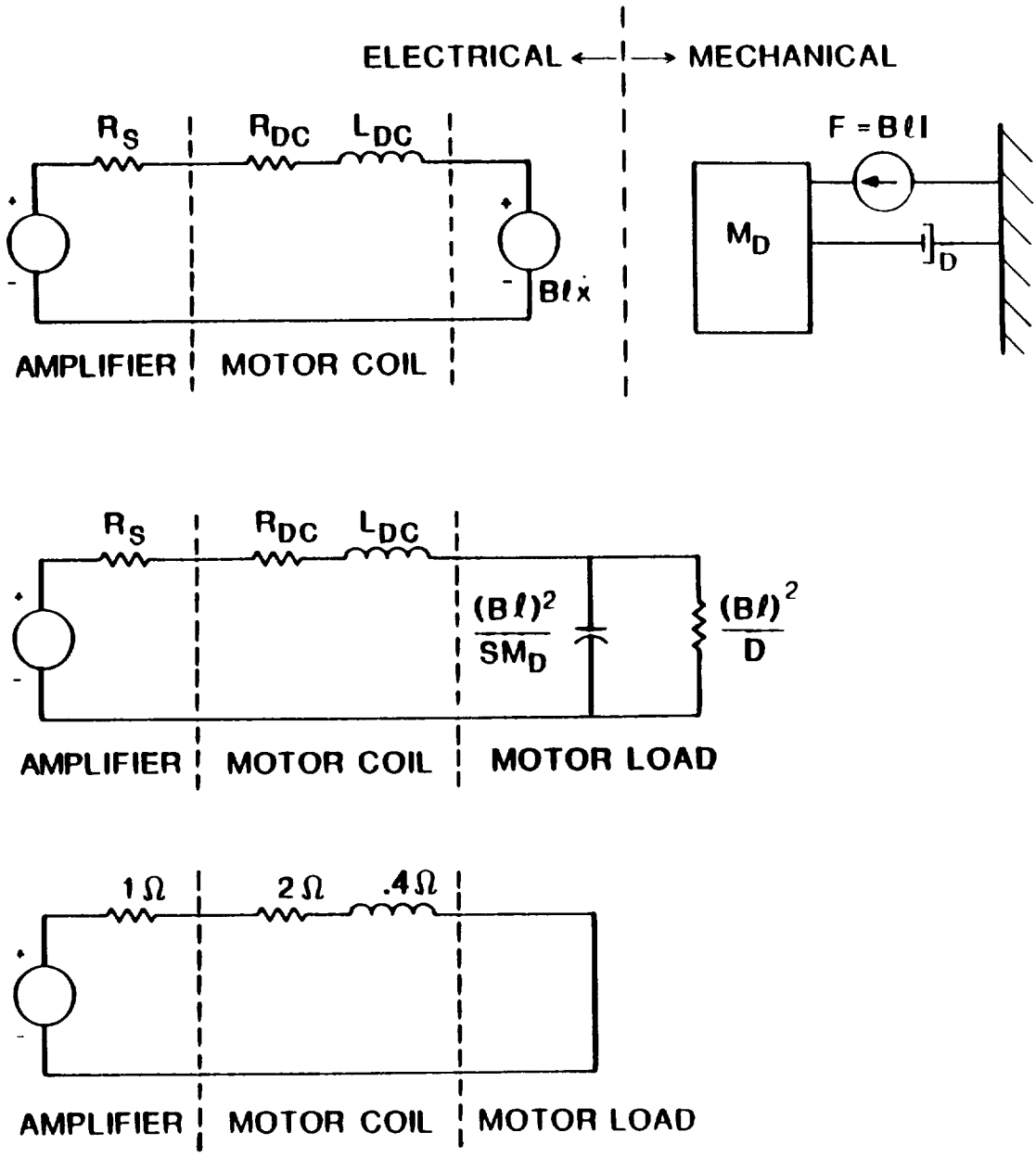

Figure 18. Derivation of effective displacer system impedance.

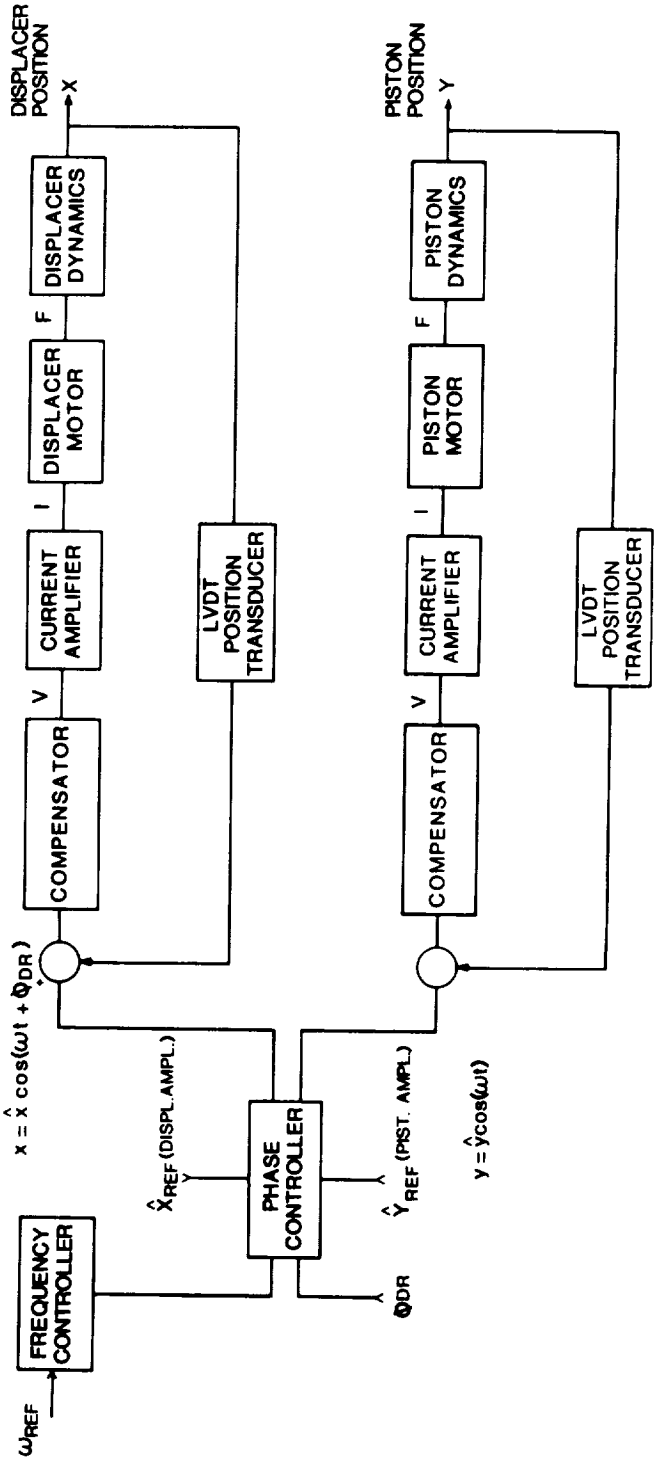

Figure 19. Piston and displacer axial control loops.

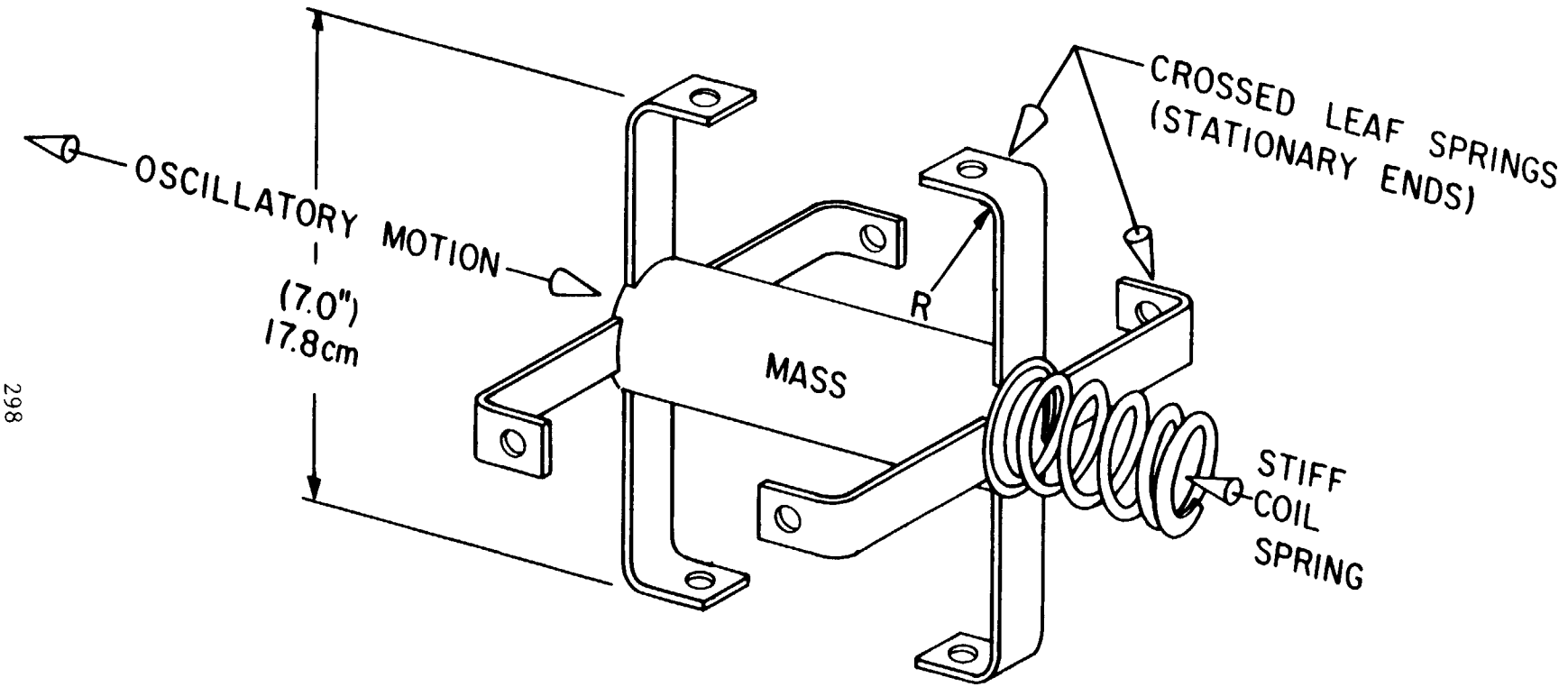

Figure 20. Schematic of vibration absorber.

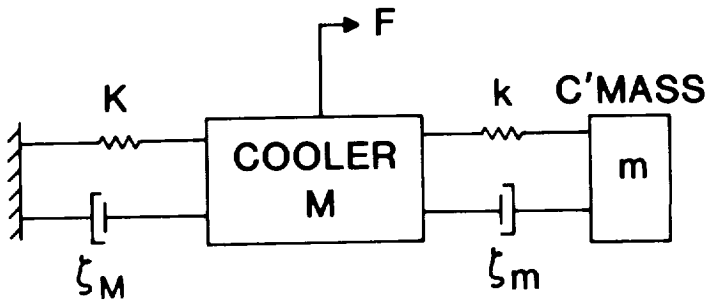

M = mass of refrigerator

K = spring constant of refrigerator mount

ζ_M = damping factor of refrigerator mount

m = mass of countermass

k = spring constant of countermass coil spring

ζ_m = damping factor of countermass coil spring

Figure 21. Vibration model of cooler/counterbalance system.

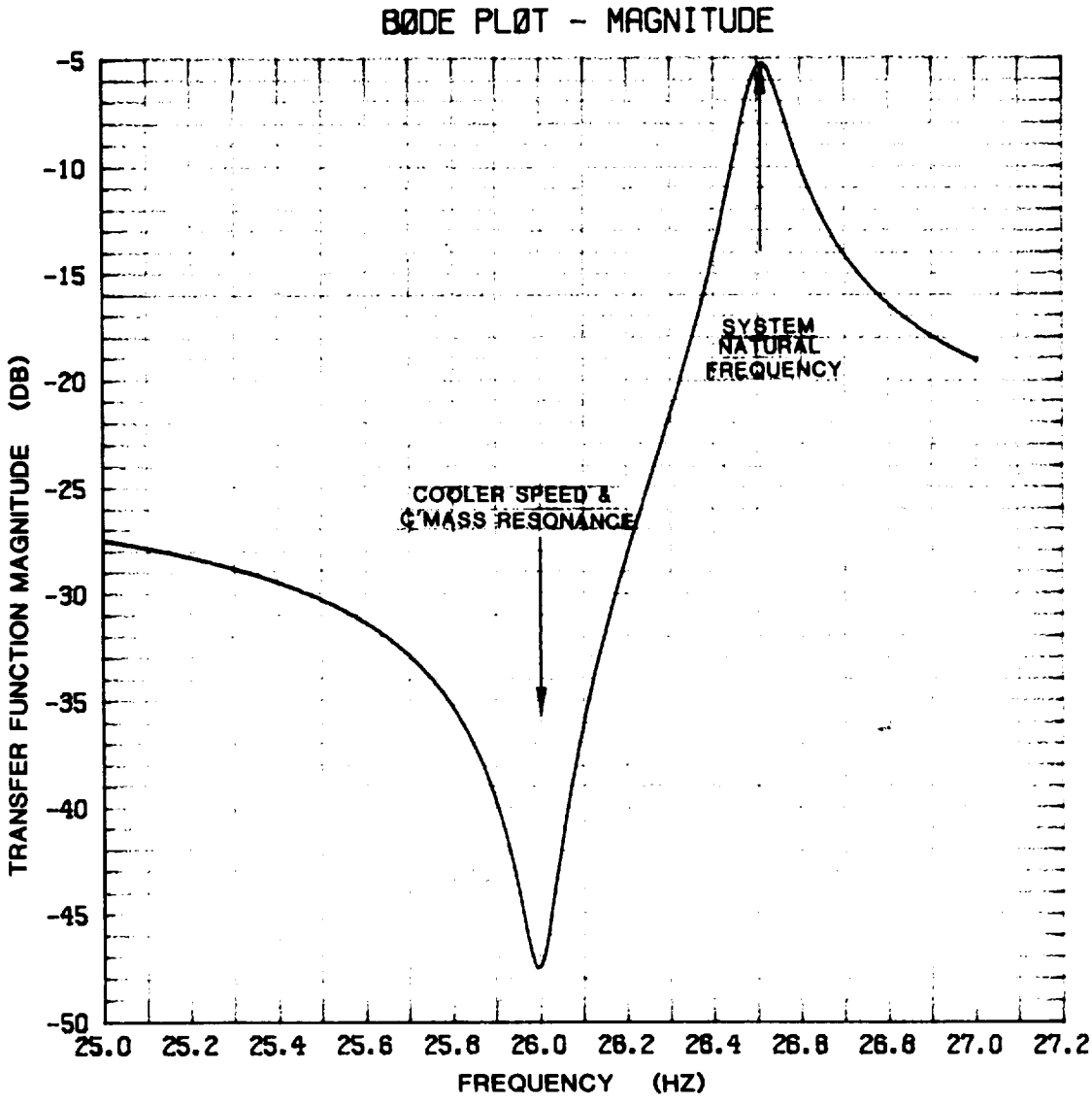

Figure 22. Calculated transmitted force imparted to refrigerator mount.

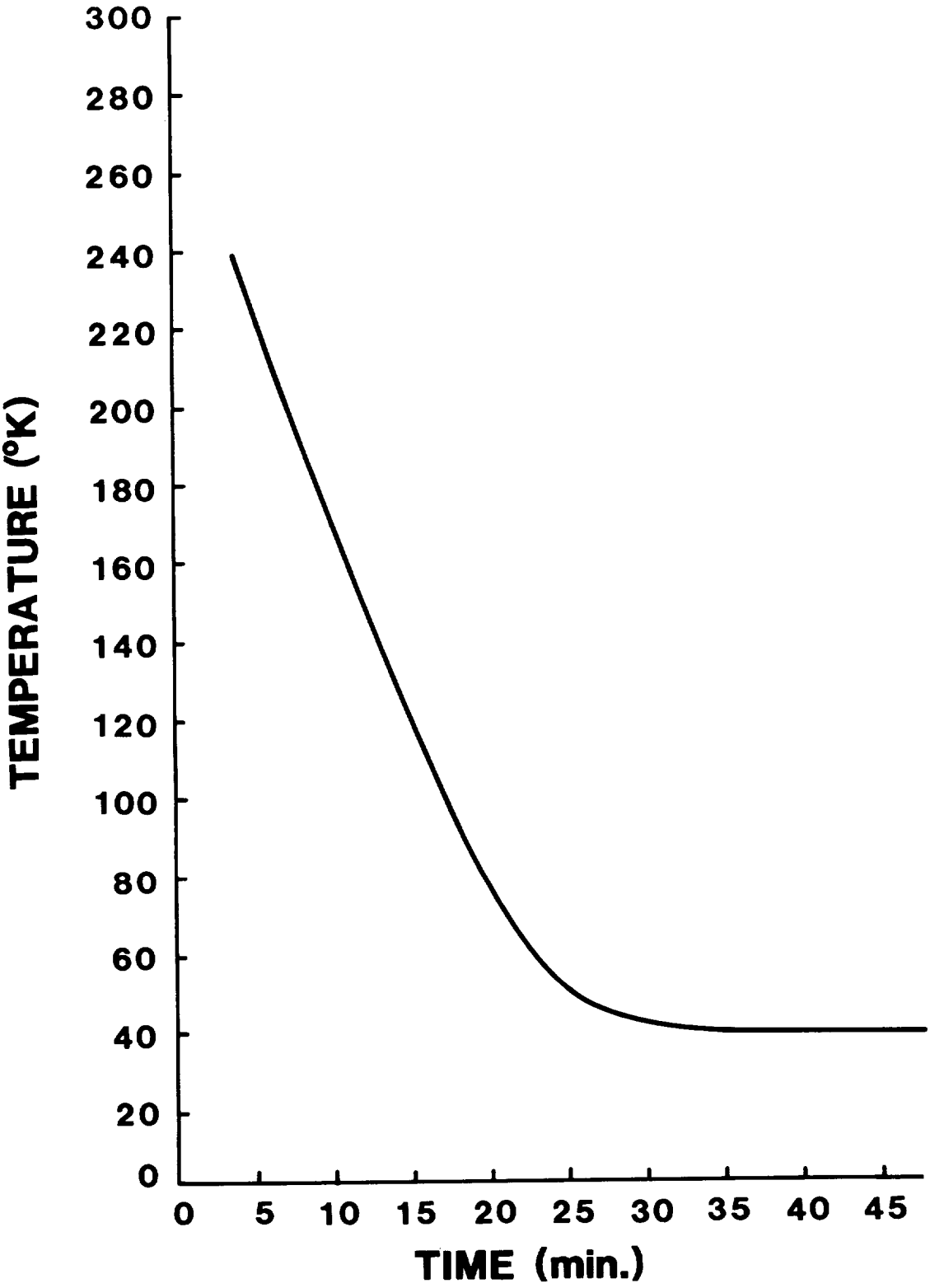

Figure 23. Cooldown time (temperature vs. time).

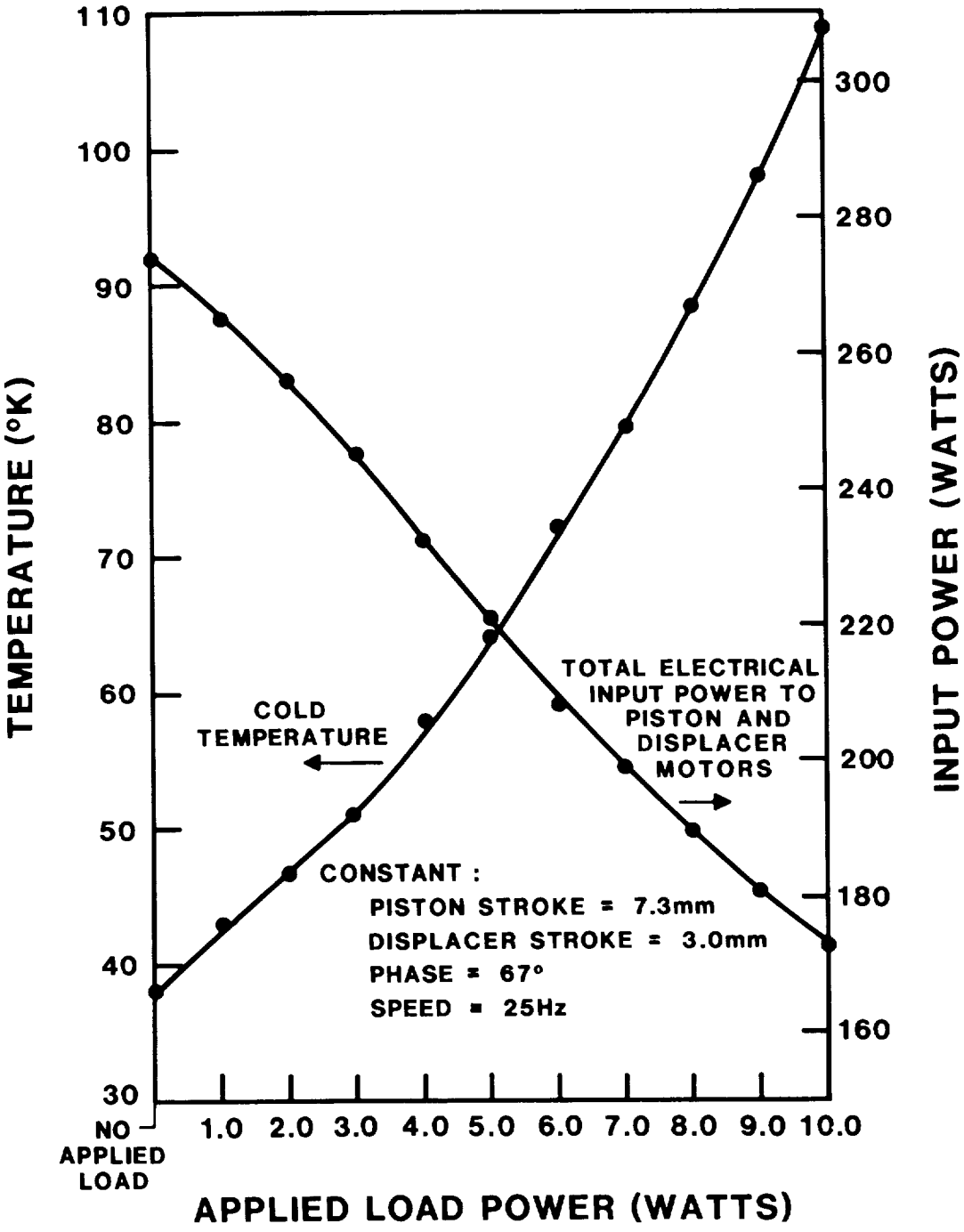

Figure 24. Load map.

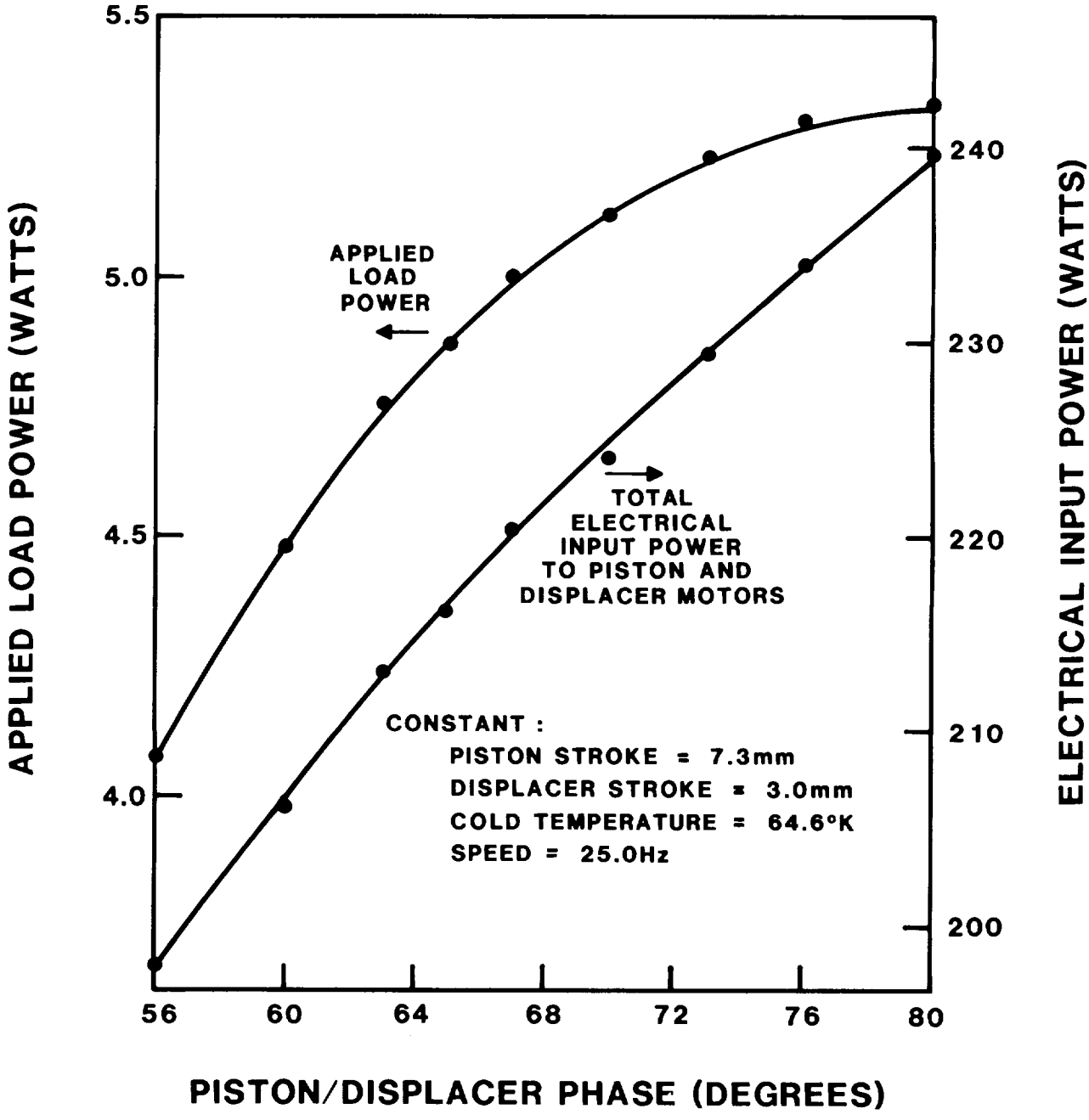

Figure 25. Parametric sensitivity piston/displacer phase.